

Fermi National Accelerator Laboratory

Submitted to *Ann. Rev. Nucl. Part. Sci.* 37: (1987)
January, 1987

EFI 86-60
Fermilab-Pub-87/15-T

HEAVY QUARK SYSTEMS

Waikwok Kwong and Jonathan L. Rosner

Enrico Fermi Institute and Department of Physics,
University of Chicago, Chicago, Illinois 60637

Chris Quigg

Fermi National Accelerator Laboratory,
P. O. Box 500, Batavia, Illinois 60510

CONTENTS

1. INTRODUCTION	1
1.1 <i>History</i>	1
1.2 <i>Scope of this article</i>	4
2. REVIEW OF THE DATA	6
2.1 <i>Preliminaries: hadrons as bound states of quarks</i>	6
2.2 <i>Survey of states</i>	6
3. THEORETICAL CONTEXT	7
3.1 <i>Quark model phenomenology for masses and widths</i>	7
3.2 <i>Quantum chromodynamics</i>	8
3.3 <i>Interpolating potentials</i>	10
3.4 <i>Spin-dependent effects</i>	11
3.5 <i>Spin-independent relativistic corrections</i>	13
3.6 <i>Coupled-channel effects</i>	14
3.7 <i>Dipole transition rates</i>	14
3.8 <i>Annihilation decays of quarkonium states</i>	15
3.9 <i>Hadronic production mechanisms</i>	18
3.10 <i>Inverse scattering</i>	19
4. THE J/ψ FAMILY AND CHARM	20
4.1 <i>Hadronic and radiative decays of J/ψ</i>	20
4.2 <i>Hadronic decays of ψ'</i>	22
4.3 <i>χ states</i>	22
4.4 <i>Spin-singlet S and P states</i>	23
4.5 <i>D wave states and prospects for further observations</i>	25
4.6 <i>States above threshold</i>	26
4.7 <i>Charmed mesons and baryons</i>	26



5. THE UPSILON FAMILY AND B-FLAVORED STATES	31
5.1 <i>Hadronic and radiative decays of Υ</i>	31
5.2 <i>Hadronic decays of higher Υ levels</i>	32
5.3 <i>χ_b states and electric dipole transitions</i>	34
5.4 <i>D wave levels</i>	36
5.5 <i>States above threshold</i>	38
5.6 <i>Flavored mesons and baryons</i>	38
6. COMPARISONS OF QUARKONIUM SPECTRA	40
6.1 <i>Flavor-independence of potential</i>	40
6.2 <i>Elementary power-law behavior</i>	40
6.3 <i>Role of heavy quarks in probing potential near $r = 0$</i>	41
6.4 <i>Flavor thresholds: counting narrow levels</i>	42
7. TOPONIUM	43
7.1 <i>Present experimental situation regarding the t quark</i>	43
7.2 <i>Prediction of levels from potential and vice versa</i>	43
7.3 <i>Weak t decays</i>	43
7.4 <i>Toponium-Z interference</i>	44
7.5 <i>Top-flavored states</i>	44
7.6 <i>Unusual short-range forces</i>	44
8. THE UNEXPECTED	45
8.1 <i>A fourth generation (b')</i>	45
8.2 <i>Scalar quarks: level structure, bounds on leptonic widths</i>	45
8.3 <i>Color sextets</i>	45
8.4 <i>Exotic quarks in superstring theories</i>	46
9. SUMMARY AND OUTLOOK	46
REFERENCES	49
TABLES	
CAPTIONS	
FIGURES	

1. INTRODUCTION AND OUTLINE

1.1 *History*

1.1.1 ATOMS, NUCLEI, POSITRONIUM AND OTHER PRE-HISTORY Two-particle bound states have played a key role in teaching us about the fundamental interactions. The hydrogen atom was one of the fertile areas from which quantum mechanics sprang seventy years ago, and it continues to illuminate the details of quantum electrodynamics. The deuteron was an essential laboratory for the development of the theory of nuclear forces. The electron-positron bound state, positronium, and corresponding bound states involving an electron and a muon, are crucial in confirming our ideas about how processes may be described in quantum field theory. In much the same manner, bound states involving heavy quark and antiquark have provided us with crucial confirmation of our present understanding of the strong interactions. These bound states and their theoretical implications form the subject of the present article. We shall also be concerned, but to a lesser extent, with bound states involving single heavy quarks.

1.1.2. LIGHT QUARK SPECTROSCOPY The strong interactions for many years resisted attempts at a quantitative treatment. A taxonomy of the hadrons, based on the quark model (1), grew up in the mid-1960's. It succeeded in describing hundreds of strongly interacting particles in terms of three elementary spin-1/2 constituents: the quarks u , d , and s , for up, down, and strange. Masses, decay rates, and magnetic moments of the mesons and baryons were systematized (2-5), but the reasons for the many successes (and occasional failures) of the quark model were not satisfactorily understood.

1.1.3. COLOR AND ASYMPTOTIC FREEDOM The requirement that quarks respect Fermi statistics led in the 1960's to the introduction of a new three-fold degree of freedom for quarks. This property (5-7), which has now become known as *color*, was

eventually recognized as a suitable strong-interaction charge on which to base a theory of interquark forces. The advent in the early 1970's of the color gauge theory (8) known as quantum chromodynamics, or *QCD*, brought the promise of a predictive theory of the strong interactions for the first time. Quarks were understood as interacting via field quanta called *gluons*, which interact with one another as well as with quarks. In electrodynamics, charge screening results in a growth of the effective charge at short distances. In contrast, in QCD the interactions among gluons (for which there is no analog in QED) lead to a diminution of the effective strong-interaction charge at short distances. This *asymptotic freedom* (9) of the strong interactions implies that perturbation theory becomes increasingly reliable at short distances, especially when these distances are small compared with the size ($1 \text{ fm} = 10^{-13} \text{ cm}$) of ordinary hadrons.

1.1.4. PSIONS AND CHARM For the light (u, d, s) quarks involved in the hadron physics of the 1960's, QCD and asymptotic freedom have mainly provided qualitative insights. The complement to asymptotic freedom in QCD is that at distances of 1 fm or larger, the strong force becomes increasingly formidable, and quarks and gluons are *confined* (10). At such distances, confinement effects dominate the dynamics. Furthermore, quark pair production becomes important: Hadrons decay readily to other lighter hadrons, and overlap and mix with one another, frustrating precise spectroscopic descriptions.

In November of 1974, a remarkably narrow resonance (dubbed the J) was discovered (11) with a mass of $3.1 \text{ GeV}/c^2$, decaying to $e^+ e^-$, in the reaction $p + \text{Be} \rightarrow e^+ e^- + \dots$. Simultaneously, the resonance was discovered (12) in the direct channel in $e^+ e^- \rightarrow \text{hadrons}$ (also to $e^+ e^-, \mu^+ \mu^-$), and was named the ψ . The dual name J/ψ has persisted. The initial evidence for it is shown in Fig. 1. The cross section for its production in $e^+ e^-$ annihilations, if integrated over center-of-mass

energy E , yields (see, e.g., (13)) its leptonic width $\Gamma_{J/\psi \rightarrow e^+ e^-}$:

$$\int dE \sigma(e^+ e^- \rightarrow J/\psi \rightarrow f; E) = \left(\frac{6\pi^2}{M_{J/\psi}^2} \right) \Gamma_{J/\psi \rightarrow e^+ e^-} \Gamma_{J/\psi \rightarrow f} / \Gamma_{tot}, \quad (1.1)$$

where the resonance may be observed in any final state f .

The J/ψ and its excitations are now understood as the bound states of the charmed quark c and its antiquark (14-18). They are the first bound system of quarks to which QCD could be expected to apply, even approximately, as a perturbative theory (16). The large mass of the c ($m_c \approx 1.5 \text{ GeV}/c^2$) sets a mass scale high enough (and correspondingly implies a bound-state size small enough) to approach the asymptotically free regime. In analogy to positronium, the $c\bar{c}$ bound states were dubbed *charmonium*, and heavy quark - antiquark bound states have come to be known as *quarkonium*. Nonrelativistic potential models (18) successfully described and predicted many properties of the new system.

Subsequently to the discovery of the J/ψ , hadrons containing a single charmed quark were found (19). Their properties had been anticipated theoretically to a large extent (14,15,18,20,21), and, in retrospect, charmed hadrons had already probably made their appearance several years earlier in cosmic ray interactions (22).

1.1.5. UPSILONS AND THEIR SIMILARITY TO PSIONS The discovery in 1977 of the Υ family of mesons was the first indication of the existence of a fifth quark, the b (beauty or bottom), with mass $m_b \approx 5 \text{ GeV}/c^2$ and charge $-1/3$. The Υ and two of its excitations were first observed in the reaction $p + (\text{Cu, Pt}) \rightarrow \mu^+ \mu^- + \dots$, as shown in Fig. 2 (23,24). The Υ family was quickly identified as a set of $b\bar{b}$ levels. Comparison of $b\bar{b}$ and $c\bar{c}$ levels showed that the interquark force was independent of the *flavor* of the quarks (25), as expected from QCD. (The flavor denotes the label u, d, s, c, b, \dots) Hadrons containing a single b quark were identified in due course (26).

1.1.6. TOP Our present understanding of the electroweak interactions implies that quarks must exist in pairs, differing in electric charge by one unit of the proton charge $|e|$. For many years, we knew of the pair u, d , and the unpaired s . The charmed quark was predicted as the partner of s , to explain the absence of strangeness-changing, charge-preserving weak interactions (20), and was subsequently found. Within three years, however, the unpaired (and unpredicted) b appeared. Its hypothetical partner, the t quark (*top* or *truth*) has yet to make a definitive appearance, but it seems required to account for the absence of flavor-changing, charge-preserving weak decays of b (27), and we expect it will be found. The toponium ($t\bar{t}$) system should be a good new laboratory for precise hadron spectroscopy based on QCD.

1.2 *Scope of this article*

We begin in §2 with a brief review of what is known experimentally about particles containing heavy quarks. We turn in §3 to the theoretical underpinnings of the spectroscopies of these particles. The J/ψ family and other hadrons containing the charmed quark occupy §4. Section 5 is devoted to the spectroscopy of hadrons containing the b quark, and §6 to a comparison of the Υ and charmonium families. The still-to-be discovered top quark, and the spectroscopy of its bound states, are treated in §7. The spectroscopic methods which have been so successful for charmonium and the Υ family can be applied to the bound states of new strongly interacting constituents, such as quarks beyond the anticipated t or spinless colored objects. Some methods for dealing with these exotic possibilities are discussed in §8. Conclusions take up §9.

The brevity of the present article requires that we cover some topics superficially and others not at all. Some subjects are treated in greater depth in general reviews (2-5,28-42). A review in this Volume (43) will treat radiative decays of J/ψ and ψ' .

Earlier reviews in this Journal are collected in (44). The papers cited in (45-47) discuss specific quantum-mechanical techniques applicable to bound states of heavy quarks. An extensive compilation of information on the coupling strength in quantum chromodynamics has been made in (48). Space limitations prevent us from discussing the sum rule method in quantum chromodynamics (49-51). Weak decays of heavy quarks, mentioned briefly by us, receive much more complete coverage in (52-55).

2. REVIEW OF THE DATA

2.1 Preliminaries: hadrons as bound states of quarks

2.1.1. MESONS A quark-antiquark ($q\bar{q}$) meson is characterized by the total spin S of the $q\bar{q}$ system ($S = 0$ or 1), the relative orbital angular momentum L , and the total angular momentum $\mathbf{J} = \mathbf{L} + \mathbf{S}$. The eigenvalues of \mathbf{J}^2 are $J(J+1)$, where J can equal $L-1$, L , or $L+1$.

We shall use extensively the spectroscopic notation $n^{2S+1}L_J$, with $L = 0$ labeled by "S," $L = 1$ by "P," $L = 2$ by "D," and so on. The radial quantum number n is equal to one plus the number of nodes of the radial wave function. Thus, the lowest S state is denoted 1S, the lowest P state 1P, the lowest D state 1D, etc.

The parity of a $q\bar{q}$ state is $P = (-1)^{L+1}$; the explicit factor of -1 arises from the opposite intrinsic parities of fermion and antifermion. A neutral $q\bar{q}$ meson is an eigenstate of the charge-conjugation operator, with eigenvalue $C = (-1)^{L+S}$. We shall often refer to a meson by the label J^{PC} .

2.1.2. BARYONS In this article we shall be concerned only with the lowest-lying states of three quarks, with total orbital angular momentum $L = 0$. These baryons thus have positive parity, and spins $J = 1/2$ or $3/2$ equal to the total quark spin S .

2.2 Survey of states

We adopt the new nomenclature of the Particle Data Group (56) for hadrons involving heavy quarks, and indicate the traditional names in parentheses when needed.

We shall be concerned with mesons and baryons containing the quarks c , b , and t . Some examples of known particles containing c and b include the $c\bar{c}$ states (Table 1 and Fig. 3), $b\bar{b}$ states (Table 2 and Fig. 4), charmed hadrons (Table 3), and b -flavored hadrons (Table 4). This rich collection of states (56–64) was unknown until about a dozen years ago. In the rest of this article we shall review what the study of these spectra has already taught us about fundamental physics, and what further we can hope to learn.

3. THEORETICAL CONTEXT

3.1 *Quark model phenomenology for hadron masses and widths*

Quarks as the constituents of hadrons were interpreted at first as convenient fictions, to be discarded once a more rigorous theory had been found, or as quasi-particles, to be used in phenomenological calculations of masses and widths based on effective Hamiltonians. We now regard them as fundamental entities, with interactions described by an underlying gauge theory. Before reviewing current understanding, however, it is helpful to recall some successes of early phenomenology with light quarks.

3.1.1. HADRON MASSES The masses of the lowest s-wave mesons and baryons may be described to within 20 MeV by the following simple picture (3), motivated by an elementary treatment (21) based on QCD: a) Add up all the quark masses m_i in the hadron. b) Add a term for the spin-spin interaction of each quark-quark or quark-antiquark pair. This term is proportional to $\sigma_i \cdot \sigma_j / m_i m_j$, where σ_i is the Pauli spin operator for the i^{th} quark. This picture totally neglects the kinetic energies or differences in binding energies of the quarks. It leads to the mass predictions shown in Table 5. Why does it work so well?

3.1.2. BARYON MAGNETIC MOMENTS By coupling the spins of quarks suitably, one can determine the magnetic moments of the hadrons containing them. For example, the magnetic moment of the proton (uud) turns out to be $\mu_p = (4\mu_u - \mu_d)/3$. That of the neutron is $\mu_n = (4\mu_d - \mu_u)/3$, so if $\mu_d = -(1/2)\mu_u$, then $\mu_n = -(2/3)\mu_p$, in good agreement with experiment. The values of the u and d quark moments μ_u and μ_d extracted from μ_p and μ_n are remarkably close to those of Dirac particles with the same masses as found in the hadron mass calculations. Why should this be so?

The above two examples are just some of the results of light-quark phenomenology which we still hope to see established on firmer ground. When we

apply similar ideas to heavy-quark physics, we begin to understand why they might hold. Our insight has been provided to a large extent by quantum chromodynamics, which we now discuss briefly.

3.2 Quantum chromodynamics

3.2.1. COLOR Just 300 MeV/c² above the neutron and proton lie three-quark states totally symmetric in spin and flavor (e.g., the Δ^{++} resonance, composed of three u quarks coupled to $J = 3/2$) which have a spatially symmetric (ground state) wave function. If the wave functions of the Δ 's are to obey Fermi statistics, they must be antisymmetric in something else, called "color." Thus baryons are composed of quarks of three different colors, and baryon wave functions are antisymmetrized in color. Color is a type of charge, coupled to a field (the *gluon* field) just as electromagnetic charge is coupled to the photon. The gauge theory of the interactions of gluons and colored quarks is known as *quantum chromodynamics*, or QCD.

The gluons couple both to each other and to quarks. The quark-gluon coupling contributes a term

$$L_{\text{int (quark-gluon)}} = -g_s \bar{\psi} \gamma_\mu \sum_a T^a A^{\mu a} \psi \quad (3.1)$$

to the interaction Lagrangian, where g_s is the (strong) coupling constant, T^a ($a = 1, \dots, 8$) are 3x3 matrices in color space, and $A^{\mu a}$ are eight gauge fields of colored gluons. The T^a may be expressed in terms of the familiar Gell-Mann matrices λ^a of $SU(3)$ as $T^a = \lambda^a/2$.

The quark-gluon interaction bears strong parallels to the electron-photon interaction in quantum electrodynamics. The gluon is massless, as is the photon. The Born term for the quark-quark or quark-antiquark interaction is thus of the familiar Coulomb ($1/r$) form, at least at short distances.

The gluon self-coupling results in a slow decrease of the effective coupling strength with decreasing distance. The distance scale is conveniently expressed in terms of its Fourier-conjugate variable Q , a characteristic momentum. By calculating the first quantum corrections to the color Coulomb potential, we find that the strong interaction analog of the fine-structure constant, $\alpha_s \equiv g_s^2/4\pi$, can be parametrized as

$$\alpha_s(Q^2) = \frac{12\pi}{(33 - 2n_f)\ln[Q^2/\Lambda^2]} \quad (3.2)$$

Here n_f is the number of fermion flavors with mass below Q , and Λ is a characteristic scale, measured in various processes (48) to be of order 200 MeV. The decrease of α_s with increasing Q^2 may be contrasted with the growth of the electromagnetic coupling at short distances, which occurs when a test charge penetrates the vacuum polarization cloud which screens a charge at large r . Because of confinement, there is no meaningful Thomson (long-distance) limit for QCD, so there is no "natural" scale on which to define α_s . For electromagnetism, on the other hand, it is conventional to define the charge in terms of its long-distance behavior.

3.2.2. SHORT DISTANCES Single gluon exchange at short distances leads to a Coulomb-like interaction

$$V(r) = -\frac{4}{3} \frac{\alpha_s(r)}{r} \quad (3.3)$$

for a quark-antiquark pair bound in a color singlet. (The factor of 4/3 comes from the group theory of $SU(3)$.) We illustrate the interaction (3.3) symbolically in Fig. 5(a). As a result of (3.2), the coupling $\alpha_s(r)$ varies logarithmically with r , so that at very short distances, gluon exchange becomes weaker. This property, known as *asymptotic freedom*, is responsible for the quasi-free behavior exhibited by quarks in hadrons

probed at very short distances by deeply inelastic scattering.

3.2.3. LONG DISTANCES The interaction (3.3) is dramatically modified in QCD at momentum scales smaller than $\Lambda \approx 200$ MeV, i.e., at distances of about 1 fm or more. Chromoelectric lines of force bunch together into a tube of approximately constant cross-sectional area, as illustrated in Fig. 5(b). By Gauss' Law, this leads to a constant, distance-independent force, or a potential

$$V(r) = kr \quad (3.4)$$

where the force constant k is about 0.14 - 0.18 GeV², or 0.7 - 0.9 GeV/fm. (The value of k may be deduced from the spectrum of light-quark mesons and baryons with high orbital excitations (65).) An indefinitely rising potential such as Eq. (3.4) permanently confines quarks so that they cannot be produced as separate entities. Up to now, no isolated quark has been observed. The form (3.4) receives theoretical support from calculations based on a spacetime lattice approach to QCD (65a).

3.3 *Interpolating potentials*

3.3.1. POWER LAWS Systems with radii larger than 1 fm, such as high orbital excitations of the light-quark hadrons, represent one extreme limit in QCD, that of long distances. In the complementary limit of short distances, a Coulomb interaction is operative. The systems of heavy quarks (c and b) that we shall discuss are more compact than 1 fm, but not so small as to be described by a Coulombic interaction alone. An effective potential

$$V(r) = Ar^\nu \quad (-1 < \nu < 1) \quad (3.5)$$

thus can interpolate between the short-distance and long-distance behavior of QCD. We shall see in §6 that a comparison of $c\bar{c}$ and $b\bar{b}$ states yields an effective power ν close to zero (45,66).

3.3.2. QCD-MOTIVATED INTERPOLATIONS Potentials motivated by perturbative QCD but incorporating the expected linear behavior at large separations have been proposed. The Fourier transform of a $1/r$ potential at small r behaves as $1/Q^2$ for large momentum transfer Q , while that of a linear potential for large r behaves as $1/Q^4$ for small Q . An expression embodying both limits which reproduces the expected logarithmic variation of the strong coupling constant for large Q^2 is (67,68)

$$V(Q^2) = \frac{16\pi}{(33-2n_f) Q^2 \ln[1+Q^2/\Lambda^2]} \quad (3.6)$$

3.4 Spin-dependent effects

The spin-independent features of quarkonium spectroscopy are well-described by the potentials just noted, or variations on them. However, various phenomena in quarkonium systems are sensitive to spin-dependences in the interquark interaction. For example, they depend on whether this interaction is of the form $V_V(r)$ that would arise from the exchange of a vector particle (a single gluon), or of the form $V_S(r)$ that would arise from an effective scalar exchange (in QCD, a collective phenomenon involving many gluons, such as the rotating flux tube illustrated in Fig. 5(b)). The vector interaction comes from the Fourier transform of a transition matrix element

$$M_{fi}^V = [\bar{u}(p_f') \gamma_\mu u(p_i')] V_V(Q^2) [\bar{u}(p_f) \gamma^\mu u(p_i)] \quad (3.7)$$

while the scalar interaction comes from

$$M_{fi}^S = [\bar{u}(p_f') u(p_i')] V_S(Q^2) [\bar{u}(p_f) u(p_i)] \quad (3.8)$$

In principle other effective interactions also are possible. Each gives rise to characteristic spin-spin, spin-orbit, and tensor forces. These are most easily found by

expanding the expressions (3.7) and (3.8) to order β^2 , where β is a characteristic quark velocity in units of c . In practice this amounts to expansion in inverse powers of quark masses. A detailed review of this method is contained in (28).

3.4.1. SPIN-SPIN INTERACTIONS The hyperfine electromagnetic interaction between a proton and an electron leads to a 1420 MHz level splitting between singlet and triplet states of atomic hydrogen. In light-quark systems, a similar spin-spin force due to single-gluon-exchange between quarks generates the splittings between the masses of the pion and the ρ resonance, the nucleon and the Δ resonance, the Σ and the Λ hyperons, and so on. The spin-spin interaction is of the form

$$V_{SS}(r) = \frac{\boldsymbol{\sigma}_1 \cdot \boldsymbol{\sigma}_2}{6 m_1 m_2} \nabla^2 V_V(r) \quad (3.9)$$

for a quark of mass m_1 and an antiquark of mass m_2 with spins described by the Pauli matrices $\boldsymbol{\sigma}_1$ and $\boldsymbol{\sigma}_2$, respectively. The expectation value of $\boldsymbol{\sigma}_1 \cdot \boldsymbol{\sigma}_2$ is +1 for a state with total quark spin $S=1$ (triplet), and -3 for $S=0$ (singlet). Only $V_V(r)$ contributes to the spin-spin interaction. If we take Eq. (3.3) for the vector interaction, and neglect the effect of ∇^2 on the slow variation of $\alpha_S(r)$ with r , we obtain a spin-spin interaction

$$V_{SS}(r) = \frac{8 \alpha_S(r) \boldsymbol{\sigma}_1 \cdot \boldsymbol{\sigma}_2}{9 m_1 m_2} \delta^3(r) \quad (3.10)$$

Because of the δ -function, this expression has nonzero matrix elements only between S-states. The absence of appreciable spin-spin splitting in states with $L > 0$ thus is a crucial test of the short-range Coulomb-like nature of the force between quarks. Such tests are just now becoming feasible for $c\bar{c}$ and $b\bar{b}$ states.

3.4.2. SPIN-ORBIT INTERACTIONS Spin-orbit forces between quarks are present for both vector and scalar interactions, but in different form. Denoting the relative orbital

angular momentum of a $q\bar{q}$ pair by \mathbf{L} , and its total spin by \mathbf{S} , we find for quarks of equal mass m :

$$V_{LS}(r) = (\mathbf{L}\cdot\mathbf{S}) (3 dV_V/dr - dV_S/dr) / (2 m^2 r) \quad (3.11)$$

For (3P_2 , 3P_1 , 3P_0) states, $\langle \mathbf{L}\cdot\mathbf{S} \rangle = (1, -1, -2)$. The vector and scalar contribution contains effects of both explicit spin-orbit interactions and Thomas precession, while only the Thomas precession is present for the scalar interaction.

3.4.3. THE TENSOR FORCE A vector interaction leads to a tensor force of the form

$$V_{tensor} = \frac{S_{12}}{12 m_1 m_2} \left(\frac{1}{r} \frac{dV_V}{dr} - \frac{d^2V_V}{dr^2} \right) \quad (3.12)$$

where $S_{12} \equiv 2 [3(\mathbf{S}\cdot\mathbf{r})(\mathbf{S}\cdot\mathbf{r}) - \mathbf{S}^2]$ has nonzero matrix elements only for $L \neq 0$.¹ Its expectation values in (3P_2 , 3P_1 , 3P_0) states are $(-2/5, 2, -4)$.

3.4.4. MODEL-INDEPENDENT DISCUSSIONS Parametrizations of spin-dependent effects in quarkonium have been given which are more general than those discussed here. We refer to the literature for details of analytic (70) and lattice-QCD (65a) treatments.

3.5. Spin-independent relativistic corrections

An expansion of the expressions (3.8) and (3.9) in inverse quark masses also yields spin-independent relativistic corrections. These introduce a flavor- (or quark-mass-) dependence into the effective interaction, even if none was present before. A typical such correction comes from expanding the total energy $(\mathbf{p}^2 + m^2)^{1/2}$ to higher order in \mathbf{p}^2 , yielding the term $-\mathbf{p}^2/8m^3$, where m is the quark mass. As we shall see in §6, a typical expectation value of the kinetic energy

¹A simple method for evaluating S_{12} may be found in (69).

$p^2/2m$ is several hundred MeV for a heavy quark - heavy antiquark bound state. A typical relativistic correction to quarkonium energy levels is then (several hundred MeV) $^2/m$, or about a hundred MeV for $c\bar{c}$ and several tens of MeV for $b\bar{b}$.

3.6. Coupled-channel effects

As the mass of a quarkonium state approaches the threshold for decay to pairs of flavored mesons, important corrections to the form of the interquark potential may arise from communication with open-flavor channels (18). These coupled-channel effects may lead to irregularities in an otherwise orderly progression of masses, leptonic widths, and other properties of the quarkonium levels given by the one-channel potential model.

3.7. Dipole transition rates

Just as in atomic physics, one can calculate electromagnetic transition rates using simple quantum mechanics. In the dipole approximation, we have

$$\text{or } \frac{\Gamma(n\ ^3S_1 \rightarrow n'\ ^3P_J + \gamma)}{\Gamma(n\ ^3P_J \rightarrow n'\ ^3S_1 + \gamma)} = \frac{4\alpha e_Q^2 E_\gamma^3}{27} (2J_f + 1) |\langle f | r | i \rangle|^2 \quad (3.13)$$

for the simplest electric dipole transitions, where J_f is the spin of the final state, and the matrix element involves normalized radial wave functions. In all of these expressions e_Q will denote the quark charge in units of the proton charge $|e|$. The simplest magnetic dipole transitions occur between 3S_1 and 1S_0 states, and are described by the rate expressions (18)

$$\text{or } \frac{\Gamma(^3S_1 \rightarrow ^1S_0 + \gamma)}{\Gamma(^1S_0 \rightarrow ^3S_1 + \gamma)} = 4\alpha e_Q^2 E_\gamma^3 (2J_f + 1) |\langle f | j_0(E_\gamma r/2) | i \rangle|^2 / 3m_Q^2, \quad (3.14)$$

where the matrix element $\langle f | j_0(E_\gamma r/2) | i \rangle$ of a spherical Bessel function between

radial wave functions reduces to one or zero in the long-wavelength limit, depending on the principal quantum numbers of the initial and final states. Finite-size corrections to the expression (3.13) also involve matrix elements of the appropriate spherical Bessel functions. Here the three-dimensional wave function $\Psi(\mathbf{r})$ is expressed in terms of spherical harmonics and (normalized) radial wave functions by

$$\Psi(\mathbf{r}) = Y_{LM}(\theta, \phi) R_{nL}(r) \quad . \quad (3.15)$$

We normalize this wave function in such a way that the integral of its square over all 3-space is 1, so that

$$\int_0^{\infty} r^2 dr [R_{nL}(r)]^2 = 1 \quad . \quad (3.16)$$

3.8. *Annihilation decays of quarkonium states*

Many quarkonium decays proceed via the annihilation of the heavy quark and antiquark, into photons and/or gluons. For s-waves, the probability of this annihilation is proportional to the square $|\Psi(0)|^2$ of the wave function at the origin. For higher partial waves $L \neq 0$, the L^{th} spatial derivative of the radial wave function $R_{nL}(r)$ at $r = 0$ governs the annihilation. Perturbative QCD expressions for annihilation decay rates in quarkonium are shown in Table 6. The decaying quarkonium state is taken to be a color singlet. [We always suppose $SU(3)$ to be the color gauge group.]

In deriving perturbative results involving gluon emission, it is assumed that the concept of an on-mass-shell gluon makes sense. In fact, the gluon must "dress" itself before emerging as hadrons. Gluons materialize as distinct jets of hadrons only when their energies exceed a few GeV, and it is for such gluons that the

perturbative results probably start to be reliable.

As mentioned at the end of §3.2.1, there is no “natural” scale on which to define α_S , so the form of the perturbative expansions in this parameter will depend on the mass scale chosen for α_S . The first-order corrections in Table 6 are all based on evaluating α_S at the mass of the decaying state, in the $\overline{\text{MS}}$ (modified minimal subtraction) renormalization scheme (48). An alternative prescription (72) for evaluating α_S at a more physically motivated (and generally smaller) scale which is widely employed leads in most cases to smaller first-order corrections. Predictions for *ratios* of rates are expected to be more reliable than individual predictions involving $|\Psi(0)|^2$, which are subject to uncertainties (74) in the definition of the nonrelativistic wave function. We now comment about individual processes.

3.8.1. ONE VIRTUAL PHOTON The decay of a 3S_1 quarkonium state into a lepton pair proceeds via a single virtual photon, as long as the initial mass M_n is sufficiently small that the contribution of a virtual Z can be ignored. The Z^0 contribution *will* be taken into account in the discussion of $t\bar{t}$ bound states. The expression (3.17) holds for any final fermion-antifermion pair $f\bar{f}$ if multiplied by e_f^2 , by the number of colors of the fermion f (three for quarks), and by a kinematic correction $(1+2m_f^2/M_n^2)(1-4m_f^2/M_n^2)^{1/2}$ for $m_f \neq 0$.

3.8.2 TWO PHOTONS a) S states. Because of charge-conjugation invariance, an s-wave quarkonium state can annihilate into two photons only from the spin-singlet state. The rate is given by Eq. (3.21). An analogous expression (with a different higher-order correction) holds for para-positronium. b) P states. The first derivative of the p-wave radial wave function at $r = 0$ governs the annihilation amplitude. The states which can decay to two real photons are 3P_0 and 3P_2 . The rates are given by Eqs. (3.23) and (3.26).

3.8.3. THREE PHOTONS As for positronium, the decay of the spin-triplet (ortho-) state leads to (at least) three photons. The rate for quarkonium is given by Eq. (3.18).

3.8.4. TWO GLUONS a) S states: Charge-conjugation invariance prevents the spin-triplet s-wave quarkonium state from decaying to two gluons. The rate for the spin-singlet state is given by Eq. (3.22). Note the large $O(\alpha_s)$ corrections.

b) P states: The rates for two-gluon decay of 3P_2 and 3P_0 states are given in Eqs. (3.24) and (3.27). In lowest-order, a common group-theoretic factor governs the ratio of two-photon to two-gluon widths for the 3P_2 , 3P_0 , and 1S_0 states:

$$\Gamma(\gamma\gamma) / \Gamma(gg) = 9 e_Q^4 \alpha^2 / 2 \alpha_s^2.$$

3.8.5. THREE GLUONS The hadronic decays of a color-singlet 3S_1 quarkonium state must proceed via at least three gluons. A single (virtual) gluon is forbidden by color symmetry, and two gluons are forbidden by charge-conjugation invariance. The three-gluon rate is given by Eq. (3.19).

Comparing (3.22) and (3.19) gives an understanding of the great stability of the J/ψ ($\Gamma_{\text{tot}} = 63 \pm 9 \text{ keV}$) in comparison with the η_c ($\Gamma_{\text{tot}} = 11 \pm 4 \text{ MeV}$). The corresponding ratio of 3γ to 2γ decay rates for the 3S_1 and 1S_0 states of positronium is $4(\pi^2-9) \alpha / 9\pi \approx 1/1115$.

3.8.6. TWO GLUONS + PHOTON The ratio α/α_s may be measured by comparing the rates for quarkonium annihilation into γgg and ggg . The result for the γgg decay is given by Eq. (3.20). Corrections to the shape of the photon spectrum also have been published (75). The mass spectrum of the two-gluon final state can be affected not only by details of how gluons turn into hadrons, but also by final-state interactions between the gluons. Consequently, the process is popular (43) in searching for quarkless hadrons ("glueballs").

3.8.7. ONE REAL AND ONE VIRTUAL GLUON A $J = 1$ particle cannot decay to two transversely polarized identical spin-1 particles. As a corollary of this result, the 3P_1 state of quarkonium cannot annihilate into two real gluons. However, the process can occur if one of the gluons is virtual and materializes into a quark-antiquark pair. The resulting rate is given by Eq. (3.25).

3.9. Hadronic production mechanisms

The processes involved in hadronic production of quarkonium states still are only partly understood. We illustrate some possible mechanisms in Fig. 6.

3.9.1. TWO-GLUON FUSION AND SUBSEQUENT ELECTROMAGNETIC DECAY When two hadrons collide, a gluon from one hadron can combine with a gluon from the other to form a C -even quarkonium $\chi(^3P_J)$ state. This state can then decay via photon emission to a 3S_1 state [Fig. 6(a)].

3.9.2. QUARK-ANTIQUARK ANNIHILATION A light quark q and antiquark \bar{q} can combine into a virtual gluon which decays into a heavy $Q\bar{Q}$ state. The $Q\bar{Q}$ pair can then radiate one or more soft gluons to reach a color singlet quarkonium state [Fig. 6(b)].

3.9.3. PROTON-ANTIPROTON ANNIHILATIONS When protons and antiprotons collide with a center-of-mass energy equal to the mass of a quarkonium state of total spin J , as shown in Fig. 6c, that state can be produced with peak cross section

$$\sigma(\bar{p}p \rightarrow [Q\bar{Q}]_J) = \pi (2J + 1) B([Q\bar{Q}]_J \rightarrow p\bar{p}) / k^{*2} \quad , \quad (3.28)$$

where k^* is the magnitude of the center-of-mass 3-momentum, and $B([Q\bar{Q}]_J \rightarrow p\bar{p})$ is the branching ratio for a quarkonium state of spin J to decay to $p\bar{p}$: more generally, $B(X \rightarrow Y) \equiv \Gamma(X \rightarrow Y)/\Gamma(X)$. This method has already been used in Experiment R-704 at the CERN ISR (76) to produce the $\chi(^3P)$ states and to uncover candidates for the charmonium 1^1P_1 and 1^1S_0 states in collisions of stored antiprotons with a hydrogen gas jet. A follow-on experiment (E-760) at the Fermilab antiproton accumulator ring (77) should achieve very high accuracy for charmonium masses and yield total widths with a precision of ± 300 keV for the χ states.

3.10. *Inverse scattering*

The interquark potential may be estimated without appeal to theoretical biases about short-distance and long-distance behavior using the inverse-scattering formalism. This procedure permits the construction of potentials with any desired spectrum of s-wave levels using only the level positions and the squares of the corresponding wave functions at the origin, $|\Psi(0)|^2$, as obtained using (3.17) from leptonic widths (25,78). These potentials provide excellent approximations to radial quarkonium potentials in the range of distances actually probed by the known levels. The method has recently been simplified by an appeal to supersymmetric quantum mechanics (79).

4. THE J/ψ FAMILY AND CHARM

4.1. Hadronic and radiative decays of J/ψ

Decays of the J/ψ provide rich information on hadrons containing light quarks. The initial state has well-defined mass, spin, parity, isospin, $SU(3)$, and charge conjugation. It is copiously produced; nearly fifteen million J/ψ 's have been accumulated in experiments at SPEAR (SLAC) (80) and DCI (Orsay) (81). We give a sample of this information, referring to the literature and (43) for details.

4.1.1. HADRONIC DECAYS OF J/ψ The hadronic decays of the J/ψ are expected to proceed mainly via three-gluon emission [Eq. (3.19)]. The ratio of rates for three-gluon and lepton pair emission [Eq. (3.17)] is

$$\frac{\Gamma(J/\psi \rightarrow ggg)}{\Gamma(J/\psi \rightarrow l^+ l^-)} = \frac{10(\pi^2 - 9)}{81\pi e_C^2} \frac{\alpha_s^3(M^2)}{\alpha^2} [1 + 10.3 \alpha_s(M^2)/\pi] , \quad (4.1)$$

if we set the J/ψ mass M equal to $2m_C$. The large $O(\alpha_s)$ correction (71) corresponds to a substantial fraction of the total rate. The gluons are not nearly energetic enough to appear as distinct jets. As a result, perturbative QCD is only a qualitative guide to the decay rate of J/ψ into hadrons. If we were to ignore the QCD correction in (4.1), we would infer $\alpha_s(M^2) \approx 0.19$ from the observed hadronic width.

When the gluons in J/ψ decay materialize into a small number of hadrons, one may hope to learn about the properties of those hadrons. The Mark III collaboration has analyzed processes of the type

$$J/\psi \rightarrow (0^- \text{ meson}) + (1^- \text{ meson}) , \quad (4.2)$$

which proceed via the graphs of Fig. 7. The 1^- mesons include ρ and ω (composed of $[u\bar{u} \pm d\bar{d}] / \sqrt{2}$) and ϕ (composed of $s\bar{s}$). The 0^- mesons include π , η , η' ,

and τ . To the extent that Fig. 7(a) dominates the decay, production of a 0^- meson opposite an ω tells the nonstrange quark content of that meson, while production opposite a ϕ tells the strange quark content. The rate may be compared with that for $J/\psi \rightarrow \rho\pi$, in which the quark content of both mesons is assumed known. The result is that while the η is almost exclusively a quark-antiquark state, with roughly half strange and half nonstrange quarks, the η' has some room (about 1/3 in probability) for a gluonic admixture (40,80).

4.1.2. RADIATIVE DECAYS Perturbative QCD, in the form of Eqs. (3.19) and (3.20), predicts that (71)

$$\frac{\Gamma(J/\psi \rightarrow \gamma gg)}{\Gamma(J/\psi \rightarrow ggg)} = \frac{16}{5} \frac{\alpha}{\alpha_s(M^2)} [1 - 5.8 \alpha_s(M^2) / \pi] . \quad (4.3)$$

The observed ratio of $(10 \pm 4)\%$ for charmonium (Ref. 82, as quoted in last of Refs. 71) corresponds to a value of $\alpha_s(M^2) = 0.29 \pm 0.08$ if we ignore the radiative corrections (which, however, are substantial).

Many interesting final states may be reached in J/ψ radiative decays (43). These are expected mainly to be those states either composed of, or with substantial couplings to, a pair of gluons. We summarize these states in Table 7. The radiative decay to a neutral pion may probe its small admixture of zero isospin. The decays to η and η' probably are sensitive to the relative gluonic admixtures in these two particles. The $f_2(1716)$ (θ) and $X(2232)$ (ξ) were first seen in radiative J/ψ decays, and the $\eta(1440)$ (ι) (seen earlier in $p\bar{p}$ annihilations) also is quite prominent. The $\eta(1440)$ and $f_2(1716)$ are candidates for gluonic bound states. The nature of the $X(2232)$ is uncertain, but it appears to have $J \geq 2$ (83). Other final states produced opposite a photon in J/ψ radiative decays (80,81) include $K\bar{K}\pi$, $\eta\pi\pi$, $\rho\rho$, $\omega\omega$, $\phi\phi$ and $\gamma\rho$. All of them but the last couple to two gluons.

4.2. Hadronic decays of ψ'

4.2.1. THE DECAYS $\psi' \rightarrow \psi \pi \pi$ AND $\psi' \rightarrow \psi \eta$ Over half of the decays of ψ' consist of hadronic transitions to the ψ , accompanied by the low-mass isoscalar systems $\pi\pi$ and η .

Semiquantitative treatments of these processes in terms of two-gluon emission by the charmed quarks exist (84).

4.2.2. DECAYS OF ψ' TO HADRONS CONTAINING LIGHT QUARKS An intriguing puzzle (85) is the relative suppression of the rates for certain hadronic ψ' decays: $B(\psi' \rightarrow \rho\pi) / B(\psi' \rightarrow \rho\pi) \leq 0.6\%$ (90% confidence level); $B(\psi' \rightarrow K^* \bar{K}) / B(\psi' \rightarrow K^* \bar{K}) \leq 2.07\%$ (90% c.l.), while the corresponding ratios for $2\pi^+ 2\pi^- \pi^0$ and $3\pi^+ 3\pi^- \pi^0$ are $(9.5 \pm 2.7)\%$ and $(13 \pm 7)\%$, respectively. Nodes in the ψ' radial wave function could be responsible for this peculiar behavior (86).

4.3. χ states

4.3.1. ELECTRIC DIPOLE TRANSITIONS The only known 3P_J states of charmonium are the χ_0 , χ_1 , and χ_2 shown in Fig. 3. They are presumably the lowest 3P states, and the only narrow ones. They were first discovered in radiative decays from the 2^3S_1 level, the $\psi(3686)$. In turn, they decay radiatively to the $J/\psi(3097)$. Measured transition rates are compared with theoretical predictions (56,87-89) in Table 8.

Purely nonrelativistic estimates of the rate for $\psi(3686) \rightarrow \gamma \chi$ are high by a factor of two to three. The exact position of the node in the 2^3S_1 wave function strongly affects the dipole matrix element $\langle 1P | r | 2S \rangle$. Relativistic distortions of the 2S and 1P wave functions substantially reduce this matrix element (88,90). Differences still remain among various relativistic treatments, but the overall agreement is satisfactory. Relativistic effects are much less important for electric dipole transitions in the $b \bar{b}$ system.

The angular distributions in the radiative $2S \rightarrow 1P$ and $1P \rightarrow 1S$ charmonium decays are in accord with expectations that the lowest multipole (electric dipole, or

E1) dominates the transitions. Studies at a slightly higher level of sensitivity than those already performed (91-93) may uncover small magnetic quadrupole (M2) contributions. The magnetic moment of the charmed quark as measured in these transitions should agree with that found in magnetic dipole, or M1, transitions.

4.3.2. TWO-GLUON AND TWO-PHOTON DECAYS Recent measurements in $p\bar{p}$ annihilations have provided the results (76) $\Gamma(\chi_2 \rightarrow \gamma\gamma) = 2.6 \pm 2.2$ keV, $\Gamma_{\text{tot}}(\chi_2) = 2.6^{+1.4}_{-1.0}$ MeV, and $\Gamma_{\text{tot}}(\chi_1) < 1.3$ MeV. The predicted ratio (73)

$$\Gamma(\chi_2 \rightarrow \gamma\gamma) / \Gamma(\chi_2 \rightarrow gg) = (8\alpha^2 / 9\alpha_s^2)(1 - 8.4 \alpha_s / \pi) \quad , \quad (4.4)$$

when combined with these measurements, would imply $\alpha_s = 0.22 \pm 0.11$ if the QCD correction were ignored. Since this correction is more than 50%, however, the convergence of the perturbation expansion cannot be guaranteed. The observed two-gluon width of the χ_2 , when compared with predictions of Eq. (3.24) and potential models (94) for the wave function, entails $\alpha_s > 0.3$. The ratio $\Gamma(\chi_1 \rightarrow gq\bar{q}) / \Gamma(\chi_2 \rightarrow gg) \approx 1.7 \alpha_s$ implied in Table 6 (using $\langle r \rangle = 3.2$ GeV⁻¹ obtained in a typical potential model (87)) only constrains $\alpha_s < 0.6$ on the basis of the data quoted above. Substantial improvements in the above data are expected in forthcoming experiments (77).

4.4. Spin-singlet S and P states

Spin-triplet charmonium states are produced copiously in e^+e^- annihilations by formation of 3S_1 levels and subsequent E1 radiative transitions to 3P_J levels, but the spin-singlet states have been more elusive. The first candidate for a 1S_0 $c\bar{c}$ level (95) appeared nearly five years after the discovery of the J/ψ , while only hints (76) of a 1P_1 state exist.

4.4.1. THE 1S_0 STATES The η'_c mentioned in Table 1 and shown in Fig. 3 as the lowest $J^{PC} = 0^{-+}$ level, is seen in magnetic dipole (M1) transitions from both the J/ψ and the

ψ' . In Table 9 we summarize the observed partial widths for these transitions and the matrix elements $\langle f | j_0(E_\gamma r/2) | i \rangle$ implied by these widths through Eq. (3.14). Also shown are matrix elements calculated on the basis of nonrelativistic wave functions. The discrepancy between the two values for J/ψ decay indicates that mixing effects and relativistic corrections appear to be important in these transitions. However, there does not yet appear to be unanimity regarding the magnitude of these effects (18,96-98).

The two-photon width of the η_c has recently been measured in $\gamma\gamma$ collisions (via $e^+e^- \rightarrow e^+e^- \eta_c$), yielding $\Gamma(\eta_c \rightarrow \gamma\gamma) = 15.0 \pm 6.3$ keV (42), and in $\bar{p}p \rightarrow \eta_c \rightarrow \gamma\gamma$, yielding 5.7^{+5}_{-4} keV (76). The average (42) is $\Gamma(\eta_c \rightarrow \gamma\gamma) = 9 \pm 4$ keV. The partial width predicted from the ratio of Eqs. (3.21) and (3.17), in the approximation $M(^3S_1) = 2 m_Q$, is (73)

$$\Gamma(\eta_c \rightarrow \gamma\gamma) = (4/3) \Gamma(J/\psi \rightarrow e^+e^-) (1 + 1.96 \alpha_s/\pi) \quad , \quad (4.5)$$

or about 7 keV for $\alpha_s = 0.22$ (42). The predicted ratio

$$\Gamma(\eta_c \rightarrow \gamma\gamma) / \Gamma(\eta_c \rightarrow gg) = (8 \alpha^2/9 \alpha_s^2) (1 - 14 \alpha_s/\pi) \quad , \quad (4.6)$$

when combined with the new $\gamma\gamma$ width and the total width of the η_c (93) of 11.5 ± 4.5 MeV, would lead to a value of $\alpha_s = 0.26 \pm 0.08$ in the absence of the QCD correction term. With the renormalization scale set at the mass of the η_c , the QCD radiative corrections are too large to permit a reliable perturbative estimate of the η_c width.

If we scale results from η_c to η_c' using the ratios of $|\Psi(0)|^2$ obtained from the corresponding 3S_1 leptonic widths, we would expect the total width of η_c' to be a few MeV. (The process $\eta_c' \rightarrow \eta_c \pi\pi$ is not expected to be a major contributor to the η_c'

total width; the partial width is estimated (84) to be ≈ 0.1 MeV.)

Further $p\bar{p}$ experiments (77) may be able to produce the η_c' and detect it via $\eta_c' \rightarrow \gamma J/\psi$. This is a "hindered" $2S \rightarrow 1S$ transition, as is the observed decay $\psi' \rightarrow \gamma \eta_c$. For $m_c = 1.8$ GeV/ c^2 , using the matrix element in Table 9, we estimate $\Gamma(\eta_c' \rightarrow \gamma J/\psi) \approx 0.5$ MeV, or a branching ratio $B(\eta_c' \rightarrow \gamma J/\psi) \approx 10^{-4}$. A more optimistic estimate of about 10^{-3} was obtained in the last of Refs. (18).

4.4.2. THE 1P_1 STATE The same $p\bar{p}$ experiment which observed the η_c also has candidate events (76) for the 1P_1 charmonium state near the mass $M(^1P_1) = [5 M(^3P_2) + 3 M(^3P_1) + M(^3P_0)]/9 \approx 3522$ MeV/ c^2 expected if the spin-spin force (3.9) were negligible for P-states. As mentioned in §3, this would confirm our notion that the spin-spin force is indeed due to a Coulomb-like interaction. Fermilab experiment E-760 (77) will be able to search more conclusively for this state.

4.5. D wave states and prospects for further observations

The $\psi(3770)$, which lies about 40 MeV above $D\bar{D}$ threshold and decays mainly to $D\bar{D}$, is a candidate for the lowest 3D_1 level of charmonium. It has a larger leptonic width than one would expect for a pure D-state, for which $\Gamma \propto |R''(0)|^2$. This is probably the result of an admixture of 2^3S_1 induced by the spin-dependent tensor force and by coupling to decay channels (18). The total width of $\psi(3770)$, 25 ± 3 MeV, is such that any electromagnetic or hadronic transitions to lower $c\bar{c}$ states are expected to occur with branching ratios of no more than a few percent (18).

One also expects 3D_2 , 3D_3 , and 1D_2 $c\bar{c}$ levels not far from the $\psi(3770)$. In one model (87) (which ignores coupled-channel effects, however) the predicted masses of these states are 3.81, 3.84, and 3.82 GeV/ c^2 , respectively, for a 3D_1 level at 3.77 GeV/ c^2 . The parities of all these levels are negative. Now, a $J^P = 2^-$ particle cannot decay to two 0^- ones, so the 3D_2 and 1D_2 $c\bar{c}$ states expected at 3.81 and

$3.82 \text{ GeV}/c^2$ cannot decay to $D\bar{D}$. Moreover, they are predicted to lie 50 or 60 MeV/c^2 below the $D^*\bar{D}$ threshold of $3.87 \text{ GeV}/c^2$. In the absence of a kinematically allowed strong decay into a pair of flavored mesons (such as makes the $\psi(3770)$ so broad), their transitions to lower $c\bar{c}$ states may be observable. In particular, the 3D_2 state may decay to $\gamma + ^3P_{2,1}$ or to $\pi\pi + J/\psi$, while the 1D_2 state may decay to $\gamma + ^1P_1$. Both states can be formed, in principle, in the direct channel of $p\bar{p}$ reactions.

4.6. States above threshold

Above flavor threshold, $c\bar{c}$ states are no longer exceptionally narrow, as shown in Table 1. The levels at 4.03 and $4.415 \text{ GeV}/c^2$ are good candidates for 3S_1 states; a level at $4.16 \text{ GeV}/c^2$ may be either a 3S_1 or 3D_1 state, or a mixture. The irregularities in the leptonic widths of the states above the charm threshold probably reflect the effects of the many hadronic channels to which such states can couple, about which little is known. It would be of particular interest to find levels which couple appreciably to $D_S\bar{D}_S$ (formerly known as $F\bar{F}$).

4.7. Charmed mesons and baryons

We have already summarized some information about charmed mesons and baryons in Table 3. Here we add a few details.

4.7.1. LIFETIMES Comparison of weak leptonic and semileptonic processes has led to the idea of Cabibbo universality, according to which, in modern language, the intrinsic strengths of the charged-current couplings to quarks and leptons are identical. This idea is embodied in the $SU(2)_L \otimes U(1)_Y$ electroweak theory, in which the charged-current couplings are determined by weak-isospin quantum numbers. Mixing among quark generations then gives couplings expressed in terms of the Cabibbo angle as $\cos\theta_C$ and $\sin\theta_C$ for the $u \leftrightarrow d$ and $u \leftrightarrow s$ transitions, in units of the electron \leftrightarrow neutrino coupling. It has been known for many years from the study of kaon and hyperon decays that in nonleptonic processes, strangeness-changing

($\Delta S=1$) interactions occur with effective strength 1, not $\sin\theta_C$. The amplification by a factor of 20 is only partially understood (99) as the work of the strong interactions. Since the discovery of the J/ψ , the hope has persisted that the study of charmed particle decays would lead to new insights into the nature of this nonleptonic enhancement. Let us examine some of the issues.

In Fig. 8 we compare lifetimes for charmed hadrons measured in a number of experiments (55) over the past few years. Several conclusions may be drawn from these values.

(a) The decay rates of hadrons containing charmed quarks are in crude accord with a free-quark picture based on the decays

$$c(1.6 \text{ GeV}/c^2) \rightarrow s(0.5 \text{ GeV}/c^2) + \begin{cases} e^+ \nu \\ \mu^+ \nu \\ u(0.3 \text{ GeV}/c^2) \quad d(0.3 \text{ GeV}/c^2) \end{cases}, \quad (4.7)$$

where we assume (20) that the weak $c \rightarrow s$ transition proceeds with the same strength as $u \rightarrow d$. The charmed quark lifetime would be about 10^{-12} s in this model. Its branching ratios to $e^+\nu$ or to $\mu^+\nu$ would each be about 20%, with nonleptonic decays making up the other 60%. In fact (56), $B(D^+ \rightarrow e^+ + \text{anything}) = (18.2 \pm 1.7)\%$, close to the naive expectation, and the D^+ lifetime is just about 10^{-12} s.

(b) Charmed quarks appear to decay more rapidly in the D^0 , D_S (F^+), and Λ_c^+ than in D^+ . In every case, the *semileptonic decay rate* $\Gamma_{\text{SL}} \equiv \Gamma(c \rightarrow s/\nu)$ is in accord with the free-quark model (4.7), as required by Cabibbo universality; it is the *nonleptonic* decay rates which are enhanced by about a factor of $2^{1/2}$ to four. Using the branching ratios quoted in (56) and lifetimes from (55), we find $\Gamma_{\text{SL}}(D^+, D^0, \Lambda_c^+) = (1.98 \pm 0.34, 1.63 \pm 0.32, 2.37 \pm 1.03) \times 10^{11} \text{ s}^{-1}$, compatible with the semileptonic rate of $1.8 \times 10^{11} \text{ s}^{-1}$ one would expect for a charmed quark of $1.6 \text{ GeV}/c^2$ in the process (4.7).

(c) The differences in nonleptonic decay rates have been ascribed to several possible mechanisms, reviewed in (52-55). The D^+ semileptonic branching ratio is close to the free-quark prediction. Thus, there is probably neither a net enhancement nor suppression (100) of D^+ nonleptonic decays. It appears that the environment of the charmed quark (100-102) can play a significant role in its nonleptonic decay rate. The study of final states in D_s and in charmed-strange baryon decays can be expected to shed further light on the mechanism of nonleptonic enhancement.

4.7.2. MASSES The simple model of hadron masses that was so successful for light-quark systems (§3.1.1) leads to the predictions shown in Table 10 for the masses of hadrons containing one charmed quark. The model is satisfactory for ordering the levels qualitatively. From the quantitative deviations, we begin to see dynamical effects. Thus, the predicted spin-averaged mass of the D_s and D_s^* is too high. The $c\bar{s}$ system has a greater reduced mass than the $c\bar{u}$ or $c\bar{d}$ system, leading to increased binding effects which are ignored in our simple model. The predicted $c\bar{s}$ hyperfine splitting is too small in comparison with that of D and D^* ; we have ignored the increase of $|\Psi(0)|^2$ with increasing reduced mass. On the other hand, the model successfully predicts $M(D^*)-M(D)=(m_s/m_c)[M(K^*)-M(K)]$.

The Λ_c was probably the first charmed particle observed (103) after the discovery of the J/ψ . The Σ_c , first seen some time ago (56,103), has recently been confirmed in e^+e^- annihilations (60). Candidate events for the charmed-strange baryons have been seen rather recently in experiments with good capability for short-track detection (62). The two Ξ_c states listed in Table 10 mix with one another slightly as a result of spin-spin interactions. Since masses in a two-state mixing problem repel one another, the lower state is expected to be somewhat lower than shown in the Table. The agreement for all known charmed baryons is certainly adequate for such a crude model.

Simple quark model considerations based on counting up $u - d$ mass differences, Coulomb self-energies, and hyperfine interactions (3,4,104) lead to the following electromagnetic mass differences, where experimental values (56,61) are shown in brackets:

$$M(D^+) - M(D^0) = 4.3 [4.7 \pm 0.3] \text{ MeV}/c^2 \quad ; \quad (4.8a)$$

$$M(D^{*+}) - M(D^{*0}) = 4.2 [2.9 \pm 1.3] \text{ MeV}/c^2 \quad ; \quad (4.8b)$$

$$M(\Sigma_c^{++}) - M(\Sigma_c^0) = 2.6 [2.5 \pm 1.0] \text{ MeV}/c^2 \quad ; \quad (4.8c)$$

$$M(\Sigma_c^{++}) - M(\Sigma_c^+) = 2.2 \text{ MeV}/c^2 \quad . \quad (4.8d)$$

Ignoring the hyperfine electromagnetic interaction, the authors of (104a) find $M(D^+) - M(D^0) = 6.7 \text{ MeV}/c^2 = M(D^{*+}) - M(D^{*0})$; $M(\Sigma_c^{++}) - M(\Sigma_c^0) = -6 \text{ MeV}/c^2$; and $M(\Sigma_c^{++}) - M(\Sigma_c^+) = -2 \text{ MeV}/c^2$.

4.7.3. HADRONIC AND ELECTROMAGNETIC DECAYS a) 3S_1 states. The D^* states can decay both to πD and to γD . The relative rates into these channels appear comparable, though one process is strong and the other electromagnetic. Quark models (18,105) predict the rates for these processes in terms of others, such as hadronic and electromagnetic decays of the $K^*(892)$. The outstanding discrepancy is a prediction $B(D^{*+} \rightarrow \gamma D^+) = 1-4\%$, to be compared with the value in (56) of $17 \pm 11\%$.

b) The Σ_c Similar quark model techniques to those just mentioned lead us to expect $\Gamma(\Sigma_c \rightarrow \Lambda_c \pi) \approx 2 \text{ MeV}$, $\Gamma(\Sigma_c^+ \rightarrow \Lambda_c \gamma) \approx 90 \text{ keV}$. We use a kinematic factor $\rho_{c.m.}^3 E(\Lambda_c) E_\pi / M(\Sigma_c)$ suggested in (18) to relate the first process to $\Sigma(1385) \rightarrow \Lambda \pi$, via a symmetry prediction for the transition matrix elements given in (106).

4.7.4. P-WAVE HADRONS CONTAINING CHARMED QUARKS The P-wave excitations 3P_2 , 3P_1 , 1P_1 , and 3P_0 of the $c\bar{u}$ and $c\bar{d}$ systems (we shall call them D^{**} here) are expected to lie somewhere between 2.2 and 2.5 GeV/c^2 . The corresponding $c\bar{s}$ excitations

should be about $100 - 150 \text{ MeV}/c^2$ heavier. Each D^{**} has decay modes characteristic of its spin and parity: ${}^3P_2 \rightarrow (\pi D^* \text{ or } \pi D)$; $({}^3P_1 \text{ or } {}^1P_1) \rightarrow \pi D^*$; ${}^3P_0 \rightarrow \pi D$. The 3P_1 and 1P_1 states are expected to mix with one another, in the manner of the two axial-vector kaons (56) $K_1(1280)$ and $K_1(1400)$. In the limit in which the charmed quark is much heavier than the u and d quarks, the mass eigenstates correspond to definite values ($1/2$ or $3/2$) of the light quark's total (orbital + spin) angular momentum (105).

A candidate for a p-wave charmed meson, the $D(2420)$, decaying to $\pi^- D^{*+}$, has been reported in one experiment (61, 107). It lies $416 \pm 6 \text{ MeV}/c^2$ above the D^{*+} , and has a width of $\Gamma[D(2420)] = 75 \pm 20 \text{ MeV}$. If the particle is real, it could be either a 1^+ or a 2^+ state. If $J^P = 1^+$, the πD decay is forbidden, whereas if $J^P = 2^+$, the πD decay rate should be about 1.5 times the πD^* rate.

The study of πD resonances could be a very fruitful source of information on the light quark - heavy quark bound state (108). In the limit that one quark is very heavy, this system becomes the relativistic one-body problem of QCD.

5. THE UPSILON FAMILY AND b -FLAVORED STATES

The family of $b\bar{b}$ bound states is our best example so far of a "hadronic hydrogen atom." Many s- and p-wave levels have been discovered, more are likely to be seen, and there is even the prospect of finding some of the predicted d-wave states. We shall mention what insights various levels of the upsilon family have provided.

5.1. Hadronic and radiative decays of Υ

5.1.1. PERTURBATIVE QCD PREDICTIONS All of the Υ decays observed so far proceed via $b\bar{b}$ annihilation. Virtual photons lead to lepton and quark pairs, while decays which can be interpreted as proceeding via γgg and ggg also have been observed. The partial widths of the Υ are summarized in Table 11.

The predicted ratio of strong and leptonic decay rates (with M_Υ taken as $2m_b$),

$$\Gamma(\Upsilon \rightarrow ggg) / \Gamma(\Upsilon \rightarrow \mu^+ \mu^-) = 10(\pi^2 - 9) \alpha_s^3(M_\Upsilon^2) / 9 \pi \alpha^2 \quad (5.1)$$

is subject to a large perturbative correction (71) of the form $[1 + 9.1 \alpha_s(M_\Upsilon^2) / \pi]$. If we ignore this correction and use the experimental value $\Gamma(\Upsilon \rightarrow ggg) / \Gamma(\Upsilon \rightarrow \mu^+ \mu^-) = 28.7 \pm 2.3$ implied by Table 11, we obtain $\alpha_s(M_\Upsilon^2) \approx 0.17$. The experimental error is insignificant compared with the theoretical one. If the energy scale $Q^* = 0.157 M_\Upsilon$ for evaluating α_s is adopted (72), the radiative correction $[1 - 14 \alpha_s(Q^*) / \pi]$ is even larger.

The process $\Upsilon \rightarrow \gamma gg$ can be separated from background for photons of greater than about half their maximum energy (109,110). The observed rate (see Table 11), when combined with the predicted ratio

$$\Gamma(\Upsilon \rightarrow \gamma gg) / \Gamma(\Upsilon \rightarrow ggg) = (4/5) [\alpha / \alpha_s(M_\Upsilon^2)] [1 - 5.5 \alpha_s(M_\Upsilon^2) / \pi] \quad (5.2)$$

then implies $\alpha_s(M_\Upsilon^2) = 0.29 \pm 0.08$ if we ignore the substantial radiative correction. Taking account of this correction, (109) quote $\alpha_s([0.157M_\Upsilon]^2) = 0.23 - 0.5$ depending on the assumed photon spectrum.

5.1.2. NEW NARROW BOSONS In principle the radiative decays of the Υ can give rise to new narrow bosons, such as Higgs bosons (111), bound states of scalar colored objects (112), or axions (113). Searches for all of these objects in Υ decays have proved negative so far (58,114,115). The level of sensitivity of Higgs boson searches is just now approaching the expected electroweak limit, corresponding to a branching ratio in the decay $\Upsilon \rightarrow \gamma + H$ of a few parts in 10^4 .

5.1.3. THE $\eta_b(1S_0)$ STATES The $^3S_1 b \bar{b}$ state (the Υ) is expected to decay to a lower-lying $^1S_0 b \bar{b}$ state (the η_b) via a magnetic dipole transition at a rate given by Eq. (3.14): for $m_b = 4.9 \text{ GeV}/c^2$,

$$\Gamma(\Upsilon \rightarrow \gamma \eta_b) = 45 \text{ eV} \times (E_\gamma / 100 \text{ MeV})^3. \quad (5.3)$$

Estimates (40, 87-89, 116) of the $\Upsilon - \eta_b$ mass difference range between 30 and 100 MeV/c^2 . Present limits (58) imply only $M(\Upsilon) - M(\eta_b) < 168 \text{ MeV}/c^2$.

We estimate using (3.14) and nonrelativistic wave functions (see also (117)) the hindered transition rate $\Gamma(\Upsilon' \rightarrow \gamma \eta_b) = 3 - 6 \text{ eV}$, corresponding to a branching ratio of about 10^{-4} . However, corrections (96-98) to (3.14) appear to be appreciable for this transition.

5.2. Hadronic decays of higher Υ levels

5.2.1. THREE-GLUON DECAYS OF $\Upsilon(2S)$ AND $\Upsilon(3S)$ The total widths of $\Upsilon(2S)$ and $\Upsilon(3S)$ may be estimated from the measured leptonic widths [see §1.1.4] and leptonic branching ratios $B_{\ell\bar{\ell}}$, of which $B_{\mu\bar{\mu}}$ is the most precisely measured. For the 2S and 3S states, a

theoretical estimate of $B_{\mu\mu}$ may usefully be obtained as follows. All decays of $\Upsilon(2S)$ and $\Upsilon(3S)$ except for radiative (E1) transitions and $\pi\pi$ emission to lower Υ levels are expected to proceed via $b\bar{b}$ annihilation. The rates for these annihilation processes are all proportional to $|\Psi_{nS}(0)|^2$. Accordingly, we may write (58)

$$B_{\mu\mu}[\Upsilon(nS)] = B_{\mu\mu}[\Upsilon(1S)] \{1 - B_{\pi\pi}[\Upsilon(nS)] - B_{E1}[\Upsilon(nS)]\}. \quad (5.4)$$

In this manner we obtain values of $(1.52 \pm 0.13)\%$ and $(1.72 \pm 0.20)\%$ for the 2S and 3S levels, to be compared with measured values (56,58) of $(1.80 \pm 0.44)\%$ (2S) and $(1.53 \pm 0.36)\%$ (3S), respectively. Using the more precise results based on Eq. (5.4), we estimate the total and partial widths and branching ratios for the 2S and 3S levels quoted in Tables 12 and 13. The branching ratios to γgg and ggg have been obtained by subtraction, and we have assumed the same $\gamma gg/ggg$ ratio as for the 1S level (Table 11). We then find $\Gamma(ggg)/\Gamma(e^+e^-) = 28.5 \pm 2.8$ (2S); 28.4 ± 4.4 (3S), in close agreement with the corresponding ratio of 28.7 ± 2.3 for the 1S level. The implied values of α_s thus are all about 0.17 in the absence of QCD corrections.

5.2.2. DECAYS $nS \rightarrow mS + \pi\pi$ The decays of excited Υ levels to lower ones can proceed via the emission of two gluons which then materialize into a $\pi\pi$ system. This mechanism also appears to be responsible for the process $\psi' \rightarrow J/\psi + \pi\pi$, which accounts for over half of the ψ' decay rate. Rates and spectra for these processes have been estimated in (84).

The $\pi\pi$ mass spectra are peaked toward the high end in $\psi' \rightarrow J/\psi + \pi\pi$, $\Upsilon(2S) \rightarrow \Upsilon(1S) + \pi\pi$, and $\Upsilon(3S) \rightarrow \Upsilon(2S) + \pi\pi$, but near its center in $\Upsilon(3S) \rightarrow \Upsilon(1S) + \pi\pi$ (59). A likely explanation would be a broad s-wave dipion resonance coupled to a pair of gluons (118).

5.2.3. THE DECAY $\Upsilon(3S) \rightarrow {}^1P_1 + \pi\pi$ One expects a 1P_1 $b\bar{b}$ state at the center of gravity

of each group of 3P_J levels, as in §4.3.2. For the lowest $b\bar{b}$ states, this corresponds to $M({}^1P_1) = [5M(\chi_{b2}) + 3M(\chi_{b1}) + M(\chi_{b0})]/9 = 9.9002 \pm 0.0007 \text{ GeV}/c^2$. In decays of $\Upsilon(3S)$ to $\pi\pi + (\text{anything})$, a weak (2.5σ) signal has been seen (59) at $M({}^1P_1) = 9.8948 \pm 0.0015 \text{ GeV}/c^2$ at a branching ratio $B[\Upsilon(3S) \rightarrow \pi\pi \Upsilon({}^1P_1)] = (0.37 \pm 0.15)\%$. As for charmonium, the close agreement between the predicted and observed masses indicates that the spin-spin splitting is very small in the lowest p-wave $b\bar{b}$ levels. This, in turn, is further evidence for the Coulomb-like nature of the force leading to the spin-spin interaction between quarks.

The branching ratio for $\Upsilon({}^1P_1) \rightarrow \gamma + \eta_b$ is expected to be around 50%, and the photon energy is expected to be around $500 \pm 30 \text{ MeV}$. The 1P_1 level thus may be a useful source of the lowest $b\bar{b}$ state.

5.3. χ_b states and electric dipole transitions

Two sets of p-wave $b\bar{b}$ levels have been discovered: a triplet around $9.9 \text{ GeV}/c^2$ (which we shall call χ_b , or 1P) and a triplet (χ_b' , or 2P) around $10.25 \text{ GeV}/c^2$. The properties of these levels are noted in more detail in Table 2. The spin-parity assignments of some of these levels are assumed from theory, but all tests performed so far (119) on the χ_b levels are compatible with the values of J^P shown and with the dominance of electric dipole transitions.

5.3.1. FINE STRUCTURE SPLITTING The masses of the χ_b levels provide valuable information on the spin-dependence of the interquark force. In the presence of vector and scalar interactions, the masses of 3P_J levels χ_J are determined by the spin-dependent interactions in §3.4.2 and 3.4.3. The spin-orbit and tensor terms probe different combinations of vector and scalar potential.

A simple model (88-90,97,120,121) based on a short-range vector interaction $V_V(r) = -(4/3) \alpha_s/r$ and a long-range scalar interaction $V_S(r) = k/r$ is compatible with present data. (A more extensive discussion has been given in (122).) The

vector interaction is expected on the basis of single-gluon exchange, while an effective scalar interaction can arise from a rotating flux tube, as mentioned in §3.4. If we define the parameter (123)

$$R \equiv [M(\chi_2) - M(\chi_1)] / [M(\chi_1) - M(\chi_0)] \quad , \quad (5.5)$$

we expect in such a model $R = 0.8 (1 - 5\lambda/16)/(1 - \lambda/8)$, where $\lambda \equiv k \langle 1/r \rangle / (\alpha_s \langle 1/r^3 \rangle)$. For a purely Coulombic force ($\lambda = 0$) one would have $R = 0.8$. If $M(\chi_2) > M(\chi_1) > M(\chi_0)$ (so the scalar interaction is not dominant), the model predicts $R < 0.8$.

We show in Table 14 the predictions of this model for $\alpha_s = 0.374$, $k = 0.18 \text{ GeV}^2$, and $m_b = 4.9 \text{ GeV}/c^2$. From both sets of p-wave levels, there is evidence for a non-Coulombic part of the interaction, and the deviations from $R = 0.8$ are as expected for a scalar long-range interaction. The question of whether there is a small long-range effective vector part of the interaction (120,122) is still unresolved (40). Arguments (87,123-6) in favor of a dominantly vector-like confining part of the potential must be evaluated in light of the successes of the scalar confinement model.

Predictions for $b\bar{b}$ fine structure parameters (87-89,120) have been discussed in (40). The quality of new experimental data will permit distinctions among these models.

5.3.2. ELECTRIC DIPOLE TRANSITION RATES If the quarkonium wavefunctions are known, one can calculate rates for electric dipole transitions among levels. These may be compared with measured transition rates provided the total widths of the decaying states are known, since it is their branching ratios that are measured directly.

One way to learn the wave functions of $b\bar{b}$ states is to construct the interquark

potential directly from bound state data (25,78,79,127). This permits the evaluation of the necessary dipole matrix elements in Eqs. (3.13); all approaches (18,87-89) agree on their values to 10%. The total widths of p-wave levels are estimated theoretically as the sum of electric dipole and hadronic partial decay rates; the latter are based on Eqs. (3.21), (3.25), and (3.22) for the $^3P_{2,1,0}$ levels, respectively.

We show the results of a comparison of predicted (127) and observed E1 transition rates in Table 15. For just one process out of 14 is the partial decay rate more than two standard deviations away from its predicted value: the transition $2^3P_1 \rightarrow \gamma + \Upsilon$. Relativistic [$O(E_\gamma/m_b)$] deviations from the simple dipole formula (3.13) for the hard photon ($E_\gamma = 763$ MeV) in this transition are estimated (87-89) to be at the 20-30% level. Notice the small predicted $3S \rightarrow 1P$ rates; the above approaches do not agree on the exact value of the matrix element, but nearly all agree it is very small.

5.4. *d wave levels*

A key test of the very existence of a potential for quarkonium systems (which could be questioned (128), if gluonic degrees of freedom are important) is its ability to predict as yet unseen aspects of the spectrum correctly. The d-wave $b\bar{b}$ states provide such a test.

5.4.1. EXPECTED MASSES Nearly all potential models agree that the lowest d-wave $b\bar{b}$ levels have centers of gravity around 10.16 (1D) and 10.44 (2D) GeV/c^2 . Predictions of the fine structure splitting differ somewhat, but most authors agree that it should be smaller than in the P states. For example, in (127) the masses (10149, 10156, 10161) and (10434, 10440, 10444) MeV/c^2 are obtained for the $1^3D_{1,2,3}$ and $2^3D_{1,2,3}$ levels in the simple model described above. These are to be compared with (10151, 10161, 10168) and (10433, 10442, 10447) MeV/c^2 (87), (10155, 10162, 10167) and (10447, 10454, 10459) MeV/c^2 (89), and (10153, 10163, 10174) and

(10444,10452,10462) MeV/c² (18).

5.4.2. SIGNATURES IN e^+e^- ANNIHILATIONS The most promising way to observe the d-wave levels appears to be to study electromagnetic transitions of the $\Upsilon(3S)$ level, as produced in e^+e^- annihilations. The expected rate of production of d-wave levels may be gauged in terms of the transitions $\Upsilon(3S) \rightarrow \gamma + \chi_b' \rightarrow \gamma + \gamma + \Upsilon(1S \text{ and/or } 2S)$, which have already been seen. It is likely that in the present sample of more than 10^5 $\Upsilon(3S)$ decays, at least 10^3 1D states have been produced. The challenge is to separate them from background.

The photons expected in the transitions $\Upsilon(3S) \rightarrow \gamma_1 + 2^3P \rightarrow \gamma_1 + \gamma_2 + 1^3D$ are expected to have a total energy lying in a narrow band: $E_{\gamma_1} + E_{\gamma_2} = 344 \pm 10$ MeV, as a result of the small fine-structure splitting in the D states. It is probably necessary to observe some signature of D-state decay: either an additional photon γ_3 with energy around 250 MeV resulting from a transition to a 1^3P state, or a pion pair + (missing mass = M_Υ). These signatures are shown in Fig. 9(a).

Direct scanning in e^+e^- annihilations with extremely high sensitivity and resolution could in principle excite the 3D_1 states. Their leptonic widths are expected to be very small (87): 1.5 eV for the 1^3D_1 (about 10^{-3} of the 1^3S_1 leptonic width, corresponding to an expected branching ratio of 3×10^{-5}), and 2.7 eV for the 2^3D_1 . Mixing with S-states, which probably affects the observed 1^3D_1 state in charmonium (the $\psi(3770)$), is expected to be much less significant for the 1^3D_1 and 2^3D_1 $b\bar{b}$ levels, since (in contrast to the $c\bar{c}$ state) they lie well below flavor threshold. Thus, coupled-channel effects are not expected to be nearly as important.

5.4.3. HADRONIC PRODUCTION It is likely that one important mechanism for 3S_1 Υ production in hadronic experiments, such as those leading to the spectrum in Fig. 2(b), is the hadronic production of *p-wave states* $\chi_{0,2}$ (since these couple to two gluons), followed by E1 decays. [The χ_1 may also be produced in this manner if one

of the gluons is virtual.] The presence of the $\Upsilon(3S)$ in the effective mass distribution of Fig. 2(b) then may signal the production of $3P\ b\ \bar{b}$ states in hadronic experiments. These states can decay not only to $\Upsilon(3S)$, but also to d-wave (particularly 2^3D) levels. The expected transitions are shown in Fig. 9(b). It may be possible to pick up the 2^3D states through their $\pi\pi\Upsilon$ decays. The 1^3D levels shown in Fig. 9(a) similarly could arise from hadronically produced 2^3P states. High-resolution studies of soft photons in hadronic experiments could shed light on decay schemes such as those shown in Fig. 9(b).

5.5. States above threshold

Just as for the charmonium levels, $b\ \bar{b}$ states are highly stable only if strong decays into pairs of flavored mesons are kinematically forbidden. Thus, the levels above the shaded line labeled by $2M(B)$ in Fig. 4 are broader than those below it, as one may see from Table 2. In light of the measured masses of B and B^* states, the $\Upsilon(4S)$ should decay only to pairs of 0^- mesons (B) each containing a b quark or antiquark and a nonstrange antiquark or quark. The decays of the higher levels (129) may be especially good sources of other b -flavored hadrons (130), such as vector mesons, baryons, and particles containing strange quarks. We turn to a brief description of such states.

5.6. Flavored mesons and baryons

5.6.1. THE $B(0^-)$ STATES Mesons containing a single b -quark (Table 4) have been reconstructed from their decays into charmed mesons (26,131). The simple model (3,4,104) described earlier for charmed meson electromagnetic mass differences predicts $M(B^0) - M(B^+) = 5.7\ \text{MeV}/c^2$, to be compared with the measured values (131) of $2.0 \pm 1.1 \pm 1.0\ \text{MeV}/c^2$ (CLEO) and $2.4 \pm 1.6\ \text{MeV}/c^2$ (ARGUS). A prediction of $4.4\ \text{MeV}/c^2$ is obtained in the last of Refs. (18).

5.6.2 VECTOR MESONS (B^*) The $B^* - B$ hyperfine splitting is expected to be proportional

to $|\Psi(0)|^2 / m_U m_b$, where $|\Psi(0)|^2$ is the square of the wave function at the origin. This wave function is expected to depend primarily on properties of the light quark, and should not be much affected if we replace the heavy b quark by another (say, c). In this manner we are led to expect that

$$\begin{aligned} M(B^*) - M(B) &= (m_c/m_b) [M(D^*) - M(D)] \\ &= (1/3) [M(D^*) - M(D)] \\ &= 50 \text{ MeV}/c^2, \end{aligned} \quad (5.6)$$

which is well verified. We predict $M(B^{*0}) - M(B^{*-}) = 5.8 \text{ MeV}/c^2$, whereas the last of Refs. (18) gives $4.4 \text{ MeV}/c^2$.

5.6.3 PREDICTED STRANGE AND BARYONIC STATES Additional states containing a b -quark may be predicted with the help of the naive quark model described in §3. We estimate $m_b - m_c$ by comparing the spin-averaged masses of the B 's and D 's:

$$m_b - m_c = \frac{3 M(B^*) + M(B)}{4} - \frac{3 M(D^*) + M(D)}{4} = 3.34 \text{ GeV}/c^2. \quad (5.7)$$

The resulting predictions for masses of the lowest b -flavored states [cf. (3); see also (132)] are shown in Fig. 10. The B_S meson is expected to be very useful in studies of mixing of neutral mesons (as in the $K-\bar{K}$ system) and CP violation (130). Indeed, same-sign dimuons produced in 630 GeV $p\bar{p}$ collisions have been interpreted (133) as evidence for $B_S-\bar{B}_S$ mixing.

6. COMPARISONS OF QUARKONIUM SPECTRA

The spectra of bound states of *different flavors* of heavy quarks appear to be described by the *same* potential. In this section we recapitulate some arguments in favor of this assertion, describe some elementary power-law properties of the potential, show how heavy quarks can provide new information at short distances, and mention expectations at larger distances (near flavor threshold).

6.1. Flavor-independence of potential

When both $c\bar{c}$ and $b\bar{b}$ bound state data became available, it was possible to construct potentials directly from these two sets of data using the inverse scattering method (25). Two such potentials based on the most recent set of masses and leptonic widths are compared in Fig. 11. They agree extremely well in the range of distances where data exist on both sets of bound states. Improved leptonic width measurements for the charmonium levels would be welcome in refining our knowledge of the $c\bar{c}$ interaction and testing flavor-independence to greater accuracy.

6.2. Elementary power-law behavior (45,66)

The similarity of $c\bar{c}$ and $b\bar{b}$ bound state spectra suggests a phenomenological power-law potential $V(r) \approx A r^\nu$ with $\nu \approx 0$. The $\nu = 0$ limit corresponds to $V(r) = C \ln(r)$, and would give spectra identical except for an overall shift. Confirming evidence is available from the level spacings in the ψ and Υ families separately, as summarized in Fig. 12. It is notable that a simple power-law interpolates between the anticipated Coulomb and linear regimes for all the known $c\bar{c}$ and $b\bar{b}$ states.

The potential $V(r) = C \ln(r)$ fits charmonium and upsilon data adequately for $C \approx 0.72$ GeV. In such a potential, all states have the same kinetic energy T . According to the virial theorem, $T = \langle (r/2)dV/dr \rangle = C/2 = 0.36$ GeV $= 2\langle p^2/2m_Q \rangle$, so

the average velocity of a quark is approximately $\langle \beta^2 \rangle = 0.36 \text{ GeV}/m_Q$. Thus we expect $\langle \beta^2 \rangle$ to be approximately 0.2 for charmed quarks, and 0.07 for b -quarks.

6.3. Role of heavy quarks in probing potential near $r = 0$

In Fig. 11 the $\Upsilon(1S)$ is more deeply bound (has a smaller mean radius) than the $\psi(1S)$. According to the Feynman-Hellmann theorem (45) $[\partial E / \partial m = -\langle T \rangle / m]$, heavier quarks probe the potential more deeply. In Fig. 13 (40) we compare predicted $c\bar{c}$, $b\bar{b}$, and $Q\bar{Q}$ levels, where Q is a hypothetical quark of mass $40 \text{ GeV}/c^2$. The *unique* information provided by the $Q\bar{Q}$ system comes from the lowest levels. The 1S level (especially its leptonic width, sensitive to $|\Psi_{1S}(0)|^2$) probes the potential at distances shorter than 0.05 fm, where $c\bar{c}$ and $b\bar{b}$ systems give little information. Potentials (87,134) with very different behavior for $r < 0.1$ fm reproduce existing $c\bar{c}$ and $b\bar{b}$ data.

As the interquark separation decreases, one expects a trend toward more Coulomb-like behavior, which may be manifested in several ways (45). First, in the limit of a pure Coulomb force, the 2S and 1P levels become degenerate. Second, the values of $|\Psi(0)|^2$ for nS levels (and hence their leptonic widths) become proportional to n^{-3} , so that $|\Psi_{2S}(0)|^2 / |\Psi_{1S}(0)|^2 \rightarrow 1/8$. Third, the spacing between 1S and 2S levels should begin to grow with increasing quark mass, reflecting the proportionality of energy levels to reduced mass in a Coulomb potential.

The first two of these trends are visible as we pass from the charmonium to the upsilon family. The 1P level is closer to the 2S (relative to the 1S - 2S spacing) in $b\bar{b}$ than in $c\bar{c}$, as we see in Fig. 12. The ratio $|\Psi_{2S}(0)|^2 / |\Psi_{1S}(0)|^2$ is 0.63 ± 0.07 for $c\bar{c}$ (characteristic of a power-law potential $V(r) \propto r^\nu$ with $\nu \approx 0.36$), and 0.50 ± 0.03 for $b\bar{b}$ (characteristic of $\nu \approx 0$). On the other hand, the 2S - 1S spacing for $b\bar{b}$ is actually slightly less than for $c\bar{c}$. This has led to the use of a phenomenological

power-law potential with a small *positive* power, in view of the expectation that level spacings in a potential behaving as r^ν should vary with quark mass m_Q as $\Delta E \propto m_Q^{-\nu/(2+\nu)}$. If QCD provides a correct short-distance description of the quark-antiquark force, the success of this description should be transitory. Detailed predictions for the 2S–1S level spacing and leptonic widths in a variety of potentials compatible with ψ and Υ data are given for heavy quarkonium systems in (40, 68, 135).

6.4. Flavor thresholds: counting narrow levels

The dissociation of a heavy quark-antiquark pair into a pair of flavored mesons should become less and less sensitive to the flavor of the heavy quark Q as $m_Q \rightarrow \infty$, occurring simply when the heavy quark pair has a given separation. This distance turns out to be about 1 fm, as shown in Fig. 11. It then becomes possible to count the number n of narrow s-wave quarkonium levels below flavor threshold (136), with the result

$$n \approx 1/4 + (1/\pi) \int dr \{m_Q [E_{TH} - V(r)]\}^{1/2} \quad , \quad (6.1)$$

where E_{TH} is the threshold energy. The integral is taken from $r = 0$ to the classical turning point, where the integrand vanishes. The only quark mass dependence arises from the explicit factor inside the square root, so that (scaling from the upsilon family) we expect $n \approx 4(m_Q/m_b)^{1/2}$. Thus, for a 40 GeV/ c^2 quark, one would expect about 10 or 11 narrow quarkonium levels below flavor threshold, as indicated in Fig. 13. As we shall see, discovery of much of this rich structure may be quite challenging.

7. TOPONIUM

7.1. *Present experimental situation regarding the t quark*

The top (t) quark, as mentioned in §1.1.6, is an as yet hypothetical charge $2/3$ partner of the b quark. Its mass is known to be larger than about $23 \text{ GeV}/c^2$. Hints of its discovery in the mass range between 30 and $50 \text{ GeV}/c^2$ seem to have been premature, but there are not yet bounds that exclude its existence in this mass range. What new physics could be learned from a $40 \text{ GeV}/c^2$ top quark? Here we give only a brief sampling; much more complete discussions have been presented in (38,68,137-139).

7.2. *Prediction of levels from potentials and vice versa*

As illustrated by the example of Fig. 13, the lowest $t\bar{t}$ levels can be expected to probe the interquark potential at distances shorter than those for which it is known at present. Predicting the properties of these levels thus requires some extrapolation of our present phenomenological knowledge. If QCD is a reliable guide, we may expect a $2S - 1S$ spacing which probably exceeds $700 \text{ MeV}/c^2$ (139) and a $1S$ leptonic width (for a $t\bar{t}$ $1S$ state at $80 \text{ GeV}/c^2$) ranging between about 4 and 8 keV (40,140). These observables discriminate between a short-distance Coulomb interaction and extrapolation of the phenomenological $V(r) \sim \ln(r)$ form.

Higher $t\bar{t}$ levels should provide information about regions of the potential already probed by $b\bar{b}$ and $c\bar{c}$. Since the bound top quark will be quite nonrelativistic, the information coming from $t\bar{t}$ in these regions of r may actually reflect the properties of the static potential more accurately.

7.3. *Weak decays of t*

Toponium may decay by annihilation into gluons, mixing with the Z^0 , strong or radiative cascades to other toponium levels, and weak decays of the t -quark. The weak decays of t increase in importance as m_t increases, as illustrated in Fig. 14.

For sufficiently high m_t , electric dipole transitions from excited S states and production of Higgs bosons via the decay $(t \bar{t}) \rightarrow \gamma + H$ occur with too small a branching ratio to study effectively [Fig. 14(c-f)].

7.4. *Toponium - Z interference*

The nS states of $(t \bar{t})$ can mix and interfere with the Z^0 , depending on their masses (38,141-143), and as a result may be more easily produced if they lie near the Z^0 . On the other hand, since they decay quite readily via the Z^0 , their transitions to other quarkonium states will occur with a smaller branching ratio.

7.5. *Top-flavored states*

7.5.1. SPIN CORRELATIONS The lightest 3S_1 state containing a single t quark is expected to undergo weak decay, carrying useful spin information (138), before it decays electromagnetically to the 1S_0 level, as a result of the small predicted hyperfine splitting.

7.5.2. CHARGED HIGGS BOSONS If there is a charged Higgs boson H^+ lighter than the t quark, the semiweak decay $t \rightarrow H^+ + b$ would dominate over any conventional semileptonic decay of t , dramatically reducing the top-quark lifetime and the canonical leptonic branching ratio $\Gamma(t \rightarrow b \ell \nu) / \Gamma(t \rightarrow \text{all}) = 1/9$. For a discussion of rates, see (144).

7.6. *Unusual short-range forces*

An enhanced coupling of neutral Higgs bosons to t quarks (145) can lead to distortions of the lowest $t \bar{t}$ levels from the expected patterns, including apparent violations of the level inequalities noted in (47).

8. THE UNEXPECTED

8.1. *A fourth generation (b')*

Much of what we have said in §6.3 applies to any heavy color triplet quark, whether of charge $2/3$ or $-1/3$. A fourth charge $-1/3$ quark b' is not excluded by present e^+e^- data above a mass of about $22.7 \text{ GeV}/c^2$ (146). A fourth generation would relax many constraints imposed by the 3-generation Kobayashi-Maskawa (KM) model (52-55) on the phenomenology of CP violation. Since the leptonic width of a $b'\bar{b}'$ state is expected to be $1/4$ that of a corresponding $t\bar{t}$ state, such quarks will be more difficult (but not impossible) to study in e^+e^- annihilations. One expects leptonic widths for the lowest 3S_1 state to be in the range of $1 - 2 \text{ keV}$ for $m_{b'} = 40 \text{ GeV}/c^2$. Scans for narrow resonances in e^+e^- annihilations should be performed with at least this sensitivity.

8.2. *Scalar quarks: level structure, bounds on leptonic widths*

Scalar quarks, or "squarks," are expected as partners of ordinary quarks on the basis of supersymmetry (147). The bound states of squarks with one another have properties which are easily calculated (112), but hard to study in the laboratory. As an example, the s-wave states are expected to be spinless, so they cannot be produced in e^+e^- annihilations. The p-wave states are expected to have very small couplings to single virtual photons. The e^+e^- cross section would grow very slowly, as β^3 (where β is the center-of-mass quark velocity) as the energy crosses threshold for squark pair production, and would approach $1/4$ the value for a corresponding spin- $1/2$ quark. Further suggestions for observing states of squarkonium have been given in (3,112,148).

8.3. *Color sextets*

Quarks of higher-color representations have been suggested in various contexts (149); in particular, color sextets should contribute twice as much to the

e^+e^- annihilation cross section as color triplets of the same charge and mass. The binding between color sextets should be stronger than between triplets, at least at short distances. It is interesting that modern superstring theories do not lead one to expect color sextet quarks, making the search for them particularly timely.

8.4. Exotic quarks in superstring theories

Popular grand unified theories with an E_6 symmetry, loosely based on superstrings, contain electroweak singlet charge $-1/3$ "h" quarks. These couple purely vectorially to the Z^0 , so the characteristic forward-backward asymmetry in e^+e^- annihilations already observed for b quarks should be absent (150).

9. SUMMARY AND OUTLOOK

In only a dozen years, the subject of heavy-quark systems has grown from its infancy to a rich spectroscopy, illuminating both the strong and electroweak interactions. The quarkonium ($Q\bar{Q}$) levels are described by a flavor-independent interaction with features of both perturbative and nonperturbative quantum chromodynamics. The number of Υ levels below flavor threshold was predicted in advance, as were numerous properties of members of the Υ family, on the basis of a nonrelativistic potential interpretation.

As one passes from $c\bar{c}$ ($\beta \approx 1/2$) to $b\bar{b}$ ($\beta \approx 1/4$) systems, a nonrelativistic description based on QCD acquires greater validity. Still heavier quarks will probe the interquark interaction almost completely freed from measurable relativistic effects.

Future electron-positron and antiproton-proton experiments will provide new data on $c\bar{c}$ and $b\bar{b}$ systems, of particular interest in the study of spin-dependent forces between quarks. Present data are converging on the notion of an effective scalar interaction at large distances, but it will be possible to test this idea in the next

few years with far greater precision. The masses of 1P_1 candidates, for which far more conclusive evidence is needed, appear to lie near the spin-averaged 3P_J values, indicating the short-range nature of the spin-spin interaction, and its origin in a Coulomb-like gluon exchange.

We also look forward to more data on quarkonium systems with orbital angular momenta greater than one. At present, only one such state (the d-wave $\psi(3772)$) is known. Antiproton-proton collisions may be able to see two quasistable $J = 2$ charmonium states around $3.815 \text{ GeV}/c^2$. Almost any flavor-independent central interquark potential describing the known quarkonium levels predicts the spin-averaged masses of the d-wave $b\bar{b}$ states to lie at 10.16 ± 0.01 (1D) and 10.44 ± 0.01 (2D) GeV/c^2 .

Mesons and baryons containing single heavy quarks are yielding new information not only on the electroweak interactions, but also on hadron physics. The hyperfine splittings between D and D^* , D_S and D_S^* , and B and B^* mesons reflect the expected interactions of quarks via their chromomagnetic moments. The first hints of p-wave excitations of D mesons have appeared; further information is eagerly awaited. Electromagnetic mass differences between charged and neutral D mesons, charged and neutral charmed baryons (Σ_c), and charged and neutral B mesons all appear to agree with expectations.

Bound states of heavier quarks (such as the anticipated top, or t) will provide a variety of information. The lowest states will probe new territory (below 0.05 fm) of the interquark force, as a result of the large mass of the t quark. The higher states are affected primarily by that range of the interquark force already studied in lighter systems, and will allow confirmation of the flavor-independence of the interaction. Relativistic corrections, important for charmonium and still perceptible for the Υ family, ought to be negligible for most $t\bar{t}$ bound states.

The possibility of more quarks (beyond the t) or other colored objects means that it is crucial to understand the bound states of heavy quarks as well as we can. By so doing, we can infer properties of the fundamental constituents (such as their masses, electric charges, and any anomalous interactions they may possess) in terms of properties of the hadrons containing these constituents.

Experimental techniques for studying heavy quark systems in the future include electron-positron colliders of modest energy (151), such as the SPEAR machine in operation at Stanford and the planned Beijing Electron-Positron Collider (BEPC), proton-antiproton collisions with precisely defined center-of-mass energy (77), and large electron-positron colliders operating at the Z^0 mass and above. Further specialized colliders, perhaps operating in the Y energy range, also are under discussion (152). The Cornell (CESR) and Hamburg (DORIS) electron-positron colliders will continue to produce stimulating results under conditions of improved luminosity.

Heavy-quark spectroscopy is at once a mature field, and one with a rich future. We look forward in the next few years to enjoying its fruits as new means become available for its study.

We wish to thank Kuang-ta Chao, E. Eichten, P. Franzini, J. Lee-Franzini, G. P. Lepage, P. Mackenzie, M. Oreglia, J. Prentice, L. Rosenberg, M. Sokoloff, and S. Stone for fruitful discussions. This work was supported in part by the United States Department of Energy under Contract No. DE-AC02-82ER40073. Fermilab is operated by Universities Research Association, Inc., under contract with the United States Department of Energy.

Literature Cited

1. Gell-Mann, M. *Phys. Lett.* 8:214-15(1964); Zweig, G. CERN reports Th.401 and 412, 1964, unpublished, and in *Proc. Int. School of Phys. "Ettore Majorana", Erice, Italy, 1964*, ed. A. Zichichi, pp. 192-234. New York/London: Academic (1965)
2. Lipkin, H. J. *Phys. Rep.* 8C:173-286(1973); Rosner, J. *Phys. Rep.* 11C:189-326 (1974); Hendry, A. W., Lichtenberg, D. B. *Rep. Prog. Phys.* 41:1707-80(1978); Close, F. *An Introduction to Quarks and Partons*. New York: Academic (1979).
3. Rosner, J. *Techniques and Concepts of High Energy Physics*, ed. T. Ferbel, pp. 1-141. New York: Plenum (1981); Gasiorowicz, S., Rosner, J. L. *Am. J. Phys.* 49:954-84(1981)
4. Quigg, C. *Gauge Theories in High Energy Physics*, ed. M. K. Gaillard and R. Stora, pp. 645-822. Amsterdam: North-Holland (1982)
5. Greenberg, O. W. *Ann. Rev. Nucl. Sci.* 28:327-86(1978)
6. Greenberg, O. W. *Phys. Rev. Lett.* 13:598-602(1964)
7. Han, M., Nambu, Y. *Phys. Rev.* 139:B1006-10(1965); Nambu, Y., *Preludes in Theoretical Physics*, ed. A. de Shalit, pp. 133-42. Amsterdam: North-Holland (1966)
8. Gross, D. J., Wilczek, F. *Phys. Rev. Lett.* 30:1343-46(1973); Politzer, H. D. *Phys. Rev. Lett.* 30:1346-49(1973)
9. Gross, D. J., Wilczek, F. *Phys. Rev. D*8:3633-52(1973); *Phys. Rev. D*9:980-93 (1974); Politzer, H. D. *Phys. Rep.* 14C:129-80(1974)
10. Jaffe, R. L. *Nature* 268:201-8(1977)
11. Aubert, J. J., et al. *Phys. Rev. Lett.* 33:1404-6(1974)
12. Augustin, J. E., et al. *Phys. Rev. Lett.* 33:1406-8(1974)
13. Renard, F. M. *Basics of Electron-Positron Collisions*, p. 123. Gif-sur-Yvette, France: Editions Frontières (1981)
14. Glashow, S. L. *Experimental Meson Spectroscopy - 1974*, ed. D. A. Garelick, pp. 387-92. New York: AIP (1974)

15. Gaillard, M. K., Lee, B. W., Rosner, J. L. *Rev. Mod. Phys.* 47:277-310 (1975)
16. Appelquist, T., and Politzer, H. D. *Phys. Rev. Lett.* 34:43-45(1975)
17. De Rújula, A. Glashow, S. L. *Phys. Rev. Lett.* 34:46-49(1975); Appelquist, T. A., De Rújula, A., Politzer, H. D., Glashow, S. L. *Phys. Rev. Lett.* 34:365-69(1975)
18. Eichten, E., et al. *Phys. Rev. Lett.* 34:369-72(1975); Eichten, E., Gottfried, K., Kinoshita, T., Lane, K. D., Yan, T. M. *Phys. Rev. Lett.* 36:500-4(1976); *Phys. Rev. D*17:3090 -3117(1978); *Phys. Rev. D*21: 313(E)(1980); *Phys. Rev. D*21:203-33(1980); Eichten, E. *Phys. Rev. D*22:1819-23(1980)
19. Goldhaber, G., et al. *Phys. Rev. Lett.* 37:255-9(1976); Peruzzi, I., et al. *Phys. Rev. Lett.* 37:569-71(1976)
20. Glashow, S. L., Iliopoulos, J., Maiani, L. *Phys. Rev. D*2:1285-92(1970)
21. De Rújula, A., Georgi, H., Glashow, S. L. *Phys. Rev. D*12:147-62(1976)
22. Niu, K., Mikumo, E., Maeda, Y. *Prog. Theor. Phys.* 46:1644-46(1971)
23. Herb, S. W., et al. *Phys. Rev. Lett.* 39: 252-55(1977); Innes, W. R., et al. *Phys. Rev. Lett.* 39:1240-42, 1640(E) (1977)
24. Brown, C. N. 2nd Aspen Winter Phys. Conf., Jan 1986, Singapore: World Scientific, 1986; Kaplan, D. M. *Quarks, Strings, Dark Matter and All the Rest*, (Proc. 7th Vanderbilt High Energy Phys. Conf., Nashville, Tenn., May 15-17, 1986), ed. R. Panvini and T. Weiler, Singapore: World Scientific (1987)
25. Quigg, C. Thacker, H. B., Rosner, J. L. *Phys. Rev. D*21:234-40 (1980); Quigg, C. Rosner, J. L. *Phys. Rev. D*23:2625-37(1981)
26. Andrews, D., et al (CLEO). *Phys. Rev. Lett.* 45:219-21(1980); Finocchiaro, G., et al (CUSB). *Phys. Rev. Lett.* 45:222-25(1980); Behrends, S., et al (CLEO). *Phys. Rev. Lett.* 50:881-4(1983)
27. Kane, G. L., Peskin, M. E. *Nucl. Phys.* B195:29-38(1982)
28. Jackson, J. D. *Weak Interactions at High Energy and the Production of New Particles* (Proc. SLAC Summer Inst. on Particle Phys., Aug. 2-13, 1976), ed. M. C. Zipf, SLAC Report No. 198, pp. 147-202. Stanford: SLAC (1976); *Proc. 1977 European Conf. on Particle Physics, Budapest, Hungary*, eds. L. Jenik, I. Montvay, pp. 603-29. Budapest: Central Inst. of Phys. (1977)

29. Chinowsky, W. *Ann. Rev. Nucl. Sci.* 27:393-464(1977)
30. Novikov, V. A., et al. *Phys. Rep.* 41C:1-133 (1978)
31. Appelquist, T., Barnett, R. M., Lane, K. *Ann. Rev. Nucl. Sci.* 28:387-499(1978)
32. Goldhaber, G., Wiss. J. E. *Ann. Rev. Nucl. Sci.* 30:337-81(1980)
33. Martin, A. *Proc. 21st Int. Conf. on High Energy Physics*, Paris, July 26-31, 1982 (*J. Phys.* 43: Colloque C-3, Suppl. 12), ed. P. Pétiau, M. Porneuf, pp. 96-101. Les Ulis, France: Les Editions de Physique (1982)
34. Martin, A. *Comm. Nucl. Part. Phys.* 16:249-66(1986)
35. Franzini, P., Lee-Franzini, J. *Ann. Rev. Nucl. Part. Sci.* 33:1-29(1983)
36. Bloom, E., Peck, C. W. *Ann. Rev. Nucl. Part. Sci.* 33:143-97(1983)
37. Eichten, E. *Proc. 11th SLAC Summer Inst. on Particle Phys., SLAC, Stanford, Calif.*, ed. P. McDonough, pp. 497-516. Stanford, Calif: SLAC (1983)
38. Eichten, E. *The Sixth Quark* (12th SLAC Summer Inst. on Particle Physics, Stanford, Calif., Jul. 23-Aug. 3, 1984), ed. P. McDonough, SLAC Report No. 281, pp.1-42
39. Peskin, M. E. *Proc. 11th SLAC Summer Inst. on Particle Phys., SLAC, Stanford, Calif.*, ed. P. McDonough, pp. 151-90. Stanford, Calif: SLAC (1983)
40. Rosner, J. *Proc. Int. Symposium on Lepton and Photon Interactions at High Energy*, Kyoto, Aug. 19-24, 1985, ed. M. Konuma, K. Takahashi, pp. 447-485. Kyoto: Kyoto University (1986)
41. Berkelman, K. *Rep. Prog. Phys.* 49:1-59(1986)
42. Cooper, S. *Proc. 23rd Int. Conf. on High Energy Physics*, Berkeley, Calif., July 16-23, 1986, SLAC-Pub-4139, Nov., 1986, to be published.
43. Hitlin, D. Toki, W. *Ann. Rev. Nucl. Part. Sci.* 37 (1987), to be published
44. Cahn, R. N., ed. *e^+e^- Annihilation: New Quarks and Leptons* (A volume in the Annual Reviews Special Collections Program). Menlo Park: Benjamin-Cummings (1985)
45. Quigg, C., Rosner, J. *Phys. Rep.* 56C:167-235(1979)
46. Grosse, H., Martin, A. *Phys. Rep.* 60C:341-92(1980)
47. Baumgartner, B. Grosse, H., Martin, A. *Phys. Lett.* 146B:363-66(1984); *Nucl.*

Phys. B254:528-42(1985)

48. Duke, D. W., Roberts, R. G. *Phys. Rep.* 120:277-368(1985)
49. Shifman, M. A. *Ann. Rev. Nucl. Part. Sci.* 33:199-233(1983)
50. Reinders, L. J., Rubinstein, H. Yazaki, S. *Phys. Rep.* 127:1-97(1985)
51. Shifman, M. A., ITEP (Moscow) preprint, May, 1986, presented at *International Symposium on Production and Decay of Heavy Hadrons*, Heidelberg, May 20-23, 1986
52. Chau, L. L. *Phys. Rep.* 95:1-94(1983)
53. Thorndike, E. H. *Ann. Rev. Nucl. Part. Sci.* 35:195-243(1985); *Proc. Int. Symposium on Lepton and Photon Interactions at High Energies*, Kyoto, Aug. 19-24, 1985, ed M. Konuma, K. Takahashi, pp. 405-45. Kyoto: Kyoto University (1986)
54. Buras, A. J., Gérard, J.-M., Rückl, R. *Nucl. Phys.* B268:16-48(1986)
55. Gilchriese, M. *Proc. 23rd Int. Conf. on High Energy Phys.*, Berkeley, Calif., July, 1986
56. Aguilar-Benitez, M., et al (Particle Data Group). *Phys. Lett.* 170B:1-350(1986)
57. Edwards, C., et al. *Phys. Rev. Lett.* 48: 70-3(1982)
58. Lee-Franzini, J., et al (CUSP). *Proc. 23rd Int. Conf. on High Energy Phys.*, Berkeley, Calif., July, 1986
59. Bowcock, T., et al (CLEO). Cornell Univ. preprint CLNS 86/740, September, 1986
60. Macfarlane, D. B., et al (ARGUS). *Proc. 23rd Int. Conf. on High Energy Phys.*, Berkeley, Calif., July 17-23, 1986
61. Schindler, R., et al (Mark III). *Proc. 23rd Int. Conf. on High Energy Phys.*, Berkeley, Calif., July 17-23, 1986
62. Biagi, S. F., et al. *Phys. Lett.* 122B:455-60(1983); *Phys. Lett.* 150B:230-4(1985); *Z. Phys.* C28:175-85(1985); Coteus, P., et al., presented at Div. of Particles and Fields meeting, Am. Phys. Soc., Salt Lake City, Utah, Jan. 14-17, 1987
63. Bebek, C., et al. (CLEO). *Proc. 23rd Int. Conf. on High Energy Phys.*, Berkeley,

Calif., July 17-23, 1986

64. Han, K., et al (CUSP). *Phys. Rev. Lett.* 55:36-39(1985)
65. Nambu, Y. *Phys. Rev. D* 10: 4262-8(1974)
- 65a. Creutz, M. *Quarks, Gluons, and Lattices*. Cambridge: Cambridge Univ. Press (1983); de Forcrand, P., Stack, J. *Phys. Rev. Lett.* 55: 1254-7(1985); Michael, C. *Phys. Rev. Lett.* 56: 1219-21(1986); Campostorini, M., Moriarty, K., Rebbi, C. *Phys. Rev. Lett.* 57: 44-7(1986); Pisarski, R. D., Stack, J. D. Fermilab report 86/122-T, Sept., 1986
66. Machacek, M., Tomozawa, Y. *Ann. Phys. (N.Y.)* 110:407-20(1978); Quigg, C., Rosner, J. *Phys. Lett.* 71:153-7(1977); Martin, A. *Phys. Lett.* 93B:338-42(1980); Richard, J. M., Taxil, P. *Ann. Phys. (N.Y.)* 150:267-286(1983)
67. Carlitz, R. D., Creamer, D.B. *Ann. Phys. (N.Y.)* 118:429-75(1979); Richardson, J. L. *Phys. Lett.* 82B:272-4(1979); Buchmüller, W. Grunberg, G., Tye, S.-H. H. *Phys. Rev. Lett.* 45:103-6(1980)
68. Buchmüller, W., Tye, S.-H. H. *Phys. Rev. D* 24:132-156(1981)
69. Landau, L. D., Lifshitz, E. M. *Quantum Mechanics*, 3rd ed., p. 95. Oxford: Pergamon (1965)
70. Eichten, E., Feinberg, F. *Phys. Rev. D* 23:2724-44(1981); Gromes, D. *Z. Phys. C* 26:401-6(1984)
71. Mackenzie, P. B., Lepage, G. P. *Phys. Rev. Lett.* 47:1244-7(1981); *Perturbative Quantum Chromodynamics (Proceedings of the Conference, Tallahassee, Fla., 1981)*, eds. D. W. Duke and J. F. Owens, pp. 176-192. New York: AIP (1981); Lepage, G. P. *Proc. 1983 Int. Symposium on Lepton and Photon Interactions at High Energies, Cornell Univ., Aug. 4-9, 1983*, eds. D. G. Cassel and D. L. Kreinick, pp. 565-592. Ithaca, N. Y.: Newman Lab. of Nucl. Studies, Cornell Univ. (1983)
72. Brodsky, S. J., Lepage, G. P., Mackenzie, P. *Phys. Rev. D* 28: 228-35(1983)
73. Barbieri, R., Gatto, R., Kögerler, R. Kunszt, Z. *Phys. Lett.* 57B:455-9 (1975); Barbieri, R., Gatto, R., Kögerler, R. *Phys. Lett.* 60B:183-8(1976); Barbieri, R.,

- Gatto, R., Remiddi, E. *Phys. Lett.* 61B:145-68(1976); Barbieri, R., Curci, G., d'Emilio, E., Remiddi, E., *Nucl. Phys.* B154:535-546(1979); Barbieri, R., Caffo, M., Gatto, R., Remiddi, E. *Phys. Lett.* 95B:93-5(1980); *Nucl. Phys.* B192:61-5(1981); Barbieri, R., Gatto, R., Remiddi, E. *Phys. Lett.* 106B:497-500(1981)
74. Poggio, E. C., Schnitzer, H. J. *Phys. Rev. D*18:1175-86(1979); *Phys. Rev. D*21:2034-35(1980)
75. Photiadis, D. M. *Phys. Lett.* 164B:160-66(1985)
76. Baglin, C., et al. *Phys. Lett.* 171B:135-41(1986)
77. Menichetti, E., *Proc. First Workshop on Antimatter Physics at Low Energy*, Fermilab, Apr. 10-12, 1986, ed. B. E. Bonner and L. S. Pinsky, pp. 95-118. Batavia, IL: Fermilab (1986)
78. Thacker, H. B., Quigg, C., Rosner, J. L. *Phys. Rev. D*18: 274-86, 287-95(1978); Schonfeld, J. F., Kwong, W., Rosner, J. L., Quigg, C., Thacker, H. B. *Ann. Phys. (N.Y.)* 128:1-28(1981); Kwong, W., Rosner, J. L., Schonfeld, J. F., Quigg, C., Thacker, H. B. *Am. J. Phys.* 48:926-30(1980)
79. Kwong, W., Rosner, J. *Prog. Theor. Phys. (Suppl.)* 86:366-76 (Festschrift volume in honor of Y. Nambu) (1986)
80. L. Köpke, et al (Mark III). *Proc. 23rd Int. Conf. on High Energy Physics*, Berkeley, Calif., July 17-23, 1986
81. Augustin, J. E., et al (DM2). Orsay preprint LAL/85-27, July, 1985, submitted to *Int. Symposium on Lepton and Photon Interactions at High Energy*, Kyoto, Aug. 19-24, 1985, ed. M. Konuma, K. Takahashi. Kyoto: Kyoto University (1986)
82. Scharre, D. L., et al (Mark II). *Phys. Rev. D*23:43-55(1981)
83. Baltrusaitis, R. M. et al (Mark III). *Phys. Rev. Lett.* 56:107-10(1986)
84. Gottfried, K. *Phys. Rev. Lett.* 40:598-601(1978); Yan, T.-M. *Phys. Rev. D*22: 1652-68(1980); Kuang, Y.-P., Yan, T.-M. *Phys. Rev. D*24:2874-85 (1981); Voloshin, M. B. Inst. of Theor. and Exp. Phys. (Moscow) Report ITEP-166-1985. 1985; Ma, J., Kuang, Y.-P. *Commun. Theor. Phys.* 5:67-78 (1986); Li, G.-Z.,

- Kuang, Y.-P. *Commun. Theor. Phys.* 5:79-88 (1986)
85. Franklin, M. E. B., et al (Mark II). *Phys. Rev. Lett.* 51:963-66(1983); Edwards, C., et al (Crystal Ball), Caltech report, 1985 (unpublished)
86. Karl, G., Roberts, W. *Phys. Lett.* 144B:263-65(1984)
87. Moxhay, P., Rosner, J. L. *Phys. Rev. D*28:1132-37(1983)
88. McClary, R., Byers, N. *Phys. Rev. D*28:1692-1705(1983)
89. Gupta, S.N., Radford, S., Repko, W. *Phys. Rev. D*26:3305-8 (1982); *Phys. Rev. D*30:2424-5 (1984); *Phys. Rev. Lett.* 55:3006 (1985); *Phys. Rev. D*31:160-63(1985); *Phys. Rev. D*34:201-6(1986)
90. Henriques, A. B., Kellett, B. H., Moorhouse, R. G. *Phys. Lett.* 64B:85-92(1976)
91. Oreglia, M. J., et al (Crystal Ball). *Phys. Rev. D*25:2259-77(1982)
92. Oreglia, M. J. Thesis, Stanford University, 1980. SLAC Report No. 236
93. Gaiser, J. E., et al (Crystal Ball). *Phys. Rev. D*34:711-21(1986)
94. Olsson, M. G., Martin, A. D., Peacock, A. W. *Phys. Rev. D*31:81-84(1985); Olsson, M. G., *Proc. First Workshop on Antimatter Physics at Low Energy*, Fermilab, Apr. 10-12, 1986, ed. B. E. Bonner and L. S. Pinsky, pp.119-30. Batavia, IL: Fermilab (1986)
95. Bloom, E. D. *Proc. 1979 Int. Symposium on Lepton and Photon Interactions at High Energy, Fermilab, 1979*, eds. T. B. W. Kirk and H. D. I. Abarbanel, pp. 92-106. Batavia, IL: Fermilab (1979)
96. Sucher, J. *Rep. Prog. Phys.* 41:1781-1838(1978); Hardekopf, G. Sucher, J. *Phys. Rev. D*25:2938-43(1982)
97. Zambetakis, V., Byers, N. *Phys. Rev. D*28:2908-11(1983); Zambetakis, V., Thesis, UCLA, 1985 (unpublished)
98. Grotch, H., Owen, D. A., Sebastian, K. J. *Phys. Rev. D*30:1924-36(1984)
99. Gaillard, M. K., Lee, B. W. *Phys. Rev. Lett.* 33:108-11 (1974); Altarelli, G., Maiani, L. *Phys. Lett.* 52B: 351-4 (1974); The idea of "6*" enhancement" for charm decays was explored in Altarelli, G., Cabibbo, N., Maiani, L. *Nucl. Phys.* B88: 285-8 (1975); *Phys. Lett.* 57B:277-80 (1975); Kingsley, R. L., Treiman, S. B., Wilczek, F., Zee, A. *Phys. Rev. D* 11: 1919-23 (1975); Einhorn, M. B.,

- Quigg, C. *Phys. Rev. D* 12: 2015-30 (1975); Ellis, J. Gaillard, M. K., Nanopoulos, D. V. *Nucl. Phys. B*100:313-28 (1975); Quigg, C. *Z. Phys. C* 4: 55-62 (1980)
100. Guberina, B. Nussinov, S., Peccei, R. D., Rückl, R. *Phys. Lett.* 89B:111-15(1979); Kobayashi, T., Yamazaki, N. *Prog. Theor. Phys.* 65:775-78(1981); Peccei, R. D., Rückl, R. *Symp. on Special Topics in Gauge Field Theories*, Ahrenshoop, E. Germany, Nov. 8-13, 1981, p. 8. Berlin: Akad. Wiss. (1981); Voloshin, M. B., Shifman, M. A. *Yad. Fiz.* 41: 187-98 (1985) [*Sov. J. Nucl. Phys.* 41:120-6 (1985)]
101. Rosen, S. P. *Phys. Rev. Lett.* 44:4-7(1980); Bander, M. Silverman, D., Soni, A. *Phys. Rev. Lett.* 44:7-9(1980); Fritzsch, H., Minkowski, P. *Phys. Lett.* 90B:455-9 (1980); Bernreuther, W., Nachtmann, O., Stech, B. *Z. Phys. C*4:257-67 (1980)
102. Barger, V., Leveille, J. P., Stevenson, P. M. *Phys. Rev. Lett.* 44:226-29(1980)
103. Cazzoli, E.G., et al. *Phys. Rev. Lett.* 34:1125-28(1975)
104. Le Yaouanc, A., Oliver, L., Pène, O., Raynal, J.-C. *Phys. Lett.* 72B:53-56(1977); Itoh, C., Minamikawa, T., Miura, K., Watanabe, T. *Prog. Theor. Phys.* 61:548-58 (1979)
- 104a. Lane, K. D., Weinberg, S. *Phys. Rev. Lett.* 37:717-9(1976)
105. De Rújula, A., Georgi, H., Glashow, S. L. *Phys. Rev. Lett.* 37:398-401 (1976); Thews, R. L., Kamal, A. N. *Phys. Rev. D*32:810-812(1985); Godfrey, S. Isgur, N. *Phys. Rev. D*32:189-231 (1985) and Univ. of Toronto preprint, 1986; Rosner, J. L. *Comm. Nucl. Part. Phys.* 16:109-30(1986)
106. Lee, B. W., Quigg, C. Rosner, J. L. *Phys. Rev. D*15:157-165(1977)
107. Albrecht, H. et al (ARGUS). *Phys. Rev. Lett.* 56:549-52(1986)
108. Schnitzer, H. J. *Phys. Rev. D*18:3482-3503(1978)
109. Csorna, S., et al (CLEO). *Phys. Rev. Lett.* 56:1222-25(1986)
110. Schamberger, R. D., et al (CUSB). *Phys. Lett.* 138B:225-29(1984)
111. Wilczek, F. *Phys. Rev. Lett.* 39:1304-6(1977); Vysotsky, M. I. *Phys. Lett.* 97B:159-62(1980); Ellis, J., Enqvist, K., Nanopoulos, D. V., Ritz, S. *Phys. Lett.* 158B:417-23(1985)

112. Krasemann, H., in G. Barbiellini et al. DESY report 79/67, unpublished (1979);
Nappi, C. R. *Phys. Rev. D*25:84-88(1982);
Tye, S. H. H., Rosenfeld, C. *Phys. Rev. Lett.* 53:2215-18(1984);
Moxhay, P., Ng, Y. J., Tye, S. H. H., *Phys. Lett.* 158B:170-74(1985)
113. Peccei, R. D., Quinn, H. R. *Phys. Rev. Lett.* 38:1440-43(1977); *Phys. Rev.*
*D*16:1791-97(1977); Weinberg, S. *Phys. Rev. Lett.* 40:223-26 (1978); Wilczek,
F. *Phys. Rev. Lett.* 40:279-82(1978)
114. Mageras, G., et al (CUSB). *Phys. Rev. Lett.* 56:2672-75(1986); Bowcock, T. et
al (CLEO). *Phys. Rev. Lett.* 56:2676-79(1986)
115. Albrecht, H. et al (ARGUS). *Z. Phys. C*29:167-73(1985); *Phys. Lett.*
179B:403-8(1986); Keh, S. et al (Crystal Ball), Schmitt, P. et al. (Crystal Ball),
Irion, J. et al (Crystal Ball), *Proc. 23rd Int. Conf. on High Energy Physics*,
Berkeley, Calif., July 16-23, 1986
116. Buchmüller, W., Ng, Y. J., Tye, S.-H. H. *Phys. Rev. D*24:3003-6(1981) (see also
(121); Igi, K., Ono, S. *Phys. Rev. D*32:232-36(1985); Frank, M., O'Donnell, P. J.
Phys. Lett. 159B:174-76(1985)
117. Rosner, J. L. *Experimental Meson Spectroscopy - 1983* (Seventh Int. Conf.,
Brookhaven), ed. S. J. Lindenbaum, pp. 461-78. New York: AIP (1984)
118. Peskin, M., private communication, and Ref (39)
119. Walk, W., et al (Crystal Ball). *Phys. Rev. D*34:2611-20(1986); Skwarnicki, T. et
al (Crystal Ball). DESY report 86/087, Aug., 1986
120. Chan, L. H. *Phys. Lett.* 71B:422-24(1977); Beavis, D., Chu, S.-Y., Desai, B. R.,
Kaus, P. *Phys. Rev. D* 20,743-47(1979); *Phys. Rev. D* 20:2345-47 (1979);
Bander, M. Silverman, D. Klima, B. Maor, U. *Phys. Rev. D*29:2038-50(1984);
Phys. Lett. 134B:258-62(1984); Ito, H. *Prog. Theor. Phys.* 74:1092-1104(1985);
75:1416-30(1986); 76:567(1986); Kinki Univ. preprint, Sept., 1986;
Yoshida-Habe, C., Iwata, K. Hirano, M. Murota, T. Tsuruda, D. *Prog. Theor.*
Phys. 73:1274-77(1985); *Prog. Theor. Phys.* 75:333-39(1986); Hokkaido Univ.
report no. EPHOU86-015, Nov., 1986; Song, X., Lin, H. Univ. of Hangzhou
preprint, 1986; Yoshida, C. *Prog. Theor. Phys.* 76:474(1986); Michael, C. *Phys.*

- Rev. Lett.* 56:1219-21 (1986); Olsson, M. G., Suchyta, C. J. Univ. of Wisconsin preprint MAD/PH/312, October, 1986
121. Buchmüller, W. *Phys. Lett.* 112B:479-82 (1982); CERN report TH. 3938/84, presented at Int. School of Exotic Atoms, Erice, Italy, Mar. 31-Apr. 6, 1984
122. Ng, Y. J., Pantaleone, J., Tye, S.-H. H. *Phys. Rev. Lett.* 55:916-19 (1985); Pantaleone, J., Tye, S.-H. H., Ng, Y. J. *Phys. Rev. D* 33:777-800 (1986)
123. Schnitzer, H. *Phys. Rev. Lett.* 35:1540-42(1975)
124. Pumplin, J., Repko, W., Sato, A. *Phys. Rev. Lett.* 35:1538-40; Eichten, E., Feinberg, F. Ref. (69)
125. Mitra, A. N. *Z. Phys. C*8:25-31 (1981); Mitra, A. N., Santhanam, I. *Z. Phys. C* 8:33-42 (1981); Faessler, A., Pfenninger, Th., Straub, U., Mitra, A. N., Univ. of Tübingen preprint, 1986.
126. Adler, S. L., Davis, A. C. *Nucl. Phys. B*244:469-91(1984); Adler, S. L. *Prog. Theor. Phys. (Suppl.)* 86:12-17 (Festschrift volume in honor of Y. Nambu) (1986); Byers, N. *Proc. 23rd Int. Conf. on High Energy Physics, Berkeley, Calif., July 16-23, 1986*
127. Kwong, W., Rosner, J. L. *D wave quarkonium states*, 1987, in preparation
128. Voloshin, M. B. *Yad. Fiz.* 36:247-55 (1982) [*Sov. J. Nucl. Phys.* 36:143-8 (1982)]
129. Lovelock, D. M. J., et al (CUSB). *Phys. Rev. Lett.* 54:377-80(1985); Besson, D., et al (CLEO). *Phys. Rev. Lett.* 54:381-84(1985)
130. Ono, S., Törnqvist, N. A., Lee-Franzini, J., Sanda, A. I. *Phys. Rev. Lett.* 55:2938-40(1985)
131. Haas, P., et al (CLEO) *Phys. Rev. Lett.* 56:2781-84(1986); Alam, M. S., et al (CLEO). *Phys. Rev. D*34:905-8(1986); Albrecht, H., et al (ARGUS). *Phys. Lett.* 162B:395-99(1985); DESY report no. 86/074, July, 1986; Macfarlane, D. B., et al (ARGUS). DESY report no. 86/067, June, 1986
132. Martin, A., Richard, J. M. CERN report TH. 4584/86, November, 1986
133. Eggert, K. et al (UA1). Univ. of Aachen preprint, 1986, to appear in Proc. Rencontre de Moriond, Les Arcs, France, Mar., 1986; Ellis, N., et al (UA1).

- Proc. 23rd Int. Conf. on High Energy Physics, Berkeley, Calif., July 16-23, 1986*
134. Lichtenberg, D. B., Wills, J. G. *Lett. Nuov. Cim.* 32:86-90(1981)
 135. Moxhay, P. J., Rosner, J. L., Quigg, C. *Phys. Rev. D*23:2638-46(1981)
 136. Eichten, E., Gottfried, K. *Phys. Lett.* 66B:286-90(1977); Quigg, C., Rosner, J. L. *Phys. Lett.* 72B:462-64(1977)
 137. Jackson, J. D., Olsen, S., Tye, S.-H. H. *Proc. 1982 DPF Summer Study on Elementary Particles and Future Facilities, Snowmass, Colo.*, ed. R. Donaldson, H. R. Gustafson, F. R. Paige, pp. 175-180. Batavia, IL: Fermilab (1982)
 138. Kuhn, J. H., Ono, S. *Z. Phys.* C21:395-402(1984); (E) C24:404(1984); Kuhn, J. H. CERN report Th. 4083/84, lectures presented at XXIV Cracow School of Theoretical Physics, Zakopane, Poland, May, 1984, *Acta Phys. Polon.* B16: 969-1006 (1985); Kuhn, J. H. *Heavy Quarks, Flavor Mixing, and CP Violation* (5th Moriond Workshop, La Plagne, France, Jan. 13-19, 1985), ed. J. Tran Thanh Van, pp.91-107. Gif-sur-Yvette, France: Editions Frontières (1985); Martin, A. D., *New Particles 1985: Proceedings* (Madison, Wis., May 8-11, 1985), ed. V. Barger, D. Cline, F. Halzen, p. 24. Singapore: World Scientific (1986); Igi, K., Ono, S. Univ. of Tokyo report UT-486, June, 1986, to appear in *Essays in Honor of the 60th Birthday of Professor Yoshio Yamaguchi*. Singapore: World Scientific (1987)
 139. Lichtenberg, D. B., Clavelli, L., Wills, J. G. *Phys. Rev. D*33:284-86 (1986)
 140. Quigg, C. *Proc. 1979 Int. Symposium on Lepton and Photon Interactions at High Energy, Fermilab, 1979*, eds. T. B. W. Kirk and H. D. I. Abarbanel, pp. 239-256. Batavia, IL: Fermilab (1979)
 141. Günsken, S. Kuhn, J. H., Zerwas, P. M. *Nucl. Phys. B* 262:393-438(1985)
 142. Franzini, P. J., Gilman, F. J. *Phys. Rev. D*32:237-46(1985)
 143. Hall, L.J., King, S.F., Sharpe, S.R. *Nucl. Phys. B*260:510-30(1985)
 144. Eichten, E., Hinchliffe, I., Lane, K. D., Quigg, C. *Phys. Rev. D*34: 1547-66 (1986)
 145. Sher, M., Silverman, D. *Phys. Rev. D*31: 95-98(1985); Abbott, L. F., Sikivie, P.,

- Wise, M. B. *Phys. Rev. D*21:1393-1403(1980); Athanasiu, G. G., Franzini, P. J., Gilman, F. J., *Phys. Rev. D*30:10-19(1985)
146. Komamiya, S. *Proc. Int. Symposium on Lepton and Photon Interactions at High Energy*, Kyoto, Aug. 19-24, 1985, ed. M. Konuma, K. Takahashi, pp. 611-659. Kyoto: Kyoto University (1986); Cornet, F., Glover, E. W. N., Hagiwara, K., Martin, A. D., Zeppenfeld, D. *Phys. Lett.* 174B:224-8 (1986)
147. Dawson, S., Eichten, E., Quigg, C. *Phys. Rev. D*31:1581-1637(1985); Haber, H., Kane, G. L., *Phys. Rep.* 117:75-263 (1985)
148. Rosner, J. *Proc. 6th Int. Symposium on High Energy Spin Physics*, Marseille, France, Sept. 12-19, 1984 (*J. Phys.* 46: Colloque C2, Suppl. 2), ed. J. Soffer, pp. C2-77-93. Les Ulis, France: Les Editions de Physique (1985)
149. Ma, E. *Phys. Lett.* 58B:442-4 (1975); Karl, G. *Phys. Rev. D*14:2374 (1976); Gell-Mann, M. *Bull. Am. Phys. Soc.* 22: 541(1977); Freedman, D. Z. *Particles and fields-1977* (Division of Particles and Fields Annual Meeting, Argonne National Laboratory), eds. P. A. Shreiner, G. W. Thomas, and A. B. Wicklund, pp. 65-75, New York: AIP (1978); Wilczek, F., Zee, A. *Phys. Rev. D*16:860-8 (1977); Giles, R. C., Tye, S.-H. H. *Phys. Lett.* 73B:30-2 (1978); Ng, Y. J., Tye, S.-H. H. *Phys. Rev. Lett.* 41:6-9 (1978); Fritzsche, H. *Phys. Lett.* 78B:611-4 (1978); Freund, P. G. O., Hill, C. T. *Phys. Rev. D*19:2755-6 (1978); *Nature* 276:250 (1978); Georgi, H., Glashow, S. L. *Nucl. Phys. B*159:29-36 (1979); Dover, C. B., Gaisser, T. K., Steigman, G. *Phys. Rev. Lett.* 42:1117-20 (1979)
150. Rosner, J. *Comm. on Nucl. Part. Phys.* 15:195-221(1986)
151. Rosner, J. *Comm. on Nucl. Part. Phys.* 14:229-244(1985)
152. Eichler, R., Nakada, T., Schubert, K. R., Weseler, S., Wille, K. Swiss Inst. for Nucl. Research preprint PR-86-13, Nov., 1986

Table 1: $c\bar{c}$ Bound States.

$^1S_0 (0^{- -})$	Name	Mass (MeV/ c^2) ^a	Γ (MeV) ^a
1^1S_0	η_c	$2981. \pm 2$	11 ± 4
2^1S_0	η_c'	$3594. \pm 5^b$	< 8 (95% C.L.) ^b

$^3S_1 (1^{- -})$	Name	Mass (MeV/ c^2)	Γ (MeV)	Γ_{ee} (keV)
1^3S_1	J/ψ	3096.9 ± 0.1	0.063 ± 0.009	4.7 ± 0.3
2^3S_1	ψ'	3686.0 ± 0.1	0.215 ± 0.040	2.1 ± 0.2
3^3S_1	ψ	$4030. \pm 5$	$52. \pm 10$	0.75 ± 0.15
$4?^3S_1^{c,d}$	ψ	$4159. \pm 20$	$78. \pm 20$	0.77 ± 0.23
$4 \text{ or } 5?^3S_1^c$	ψ	$4415. \pm 6$	$43. \pm 20$	0.47 ± 0.10

$1^3P_J (J^{++})$	Name	Mass (MeV/ c^2)	Γ (MeV)
3P_0	χ_0	3414.9 ± 1.1	$13\text{--}21^e$
3P_1	χ_1	3510.7 ± 0.5	< 1.3 (90% C.L.) ^f
3P_2	χ_2	3556.3 ± 0.4	$2.6^{+1.4}_{-1.0}$ ^f

$^3D_1 (1^{- -})$	Name	Mass (MeV/ c^2)	Γ (MeV)
1^3D_1	ψ	3769.9 ± 2.4	25 ± 3

^a All properties are from Ref. (56) unless otherwise indicated.

^b Ref. (57)

^c 3S_1 states above charm threshold may be substantially mixed with 3D_1 states.

^d Possible 3D_1 , if $\psi(4415)$ is identified as 4^3S_1 .

^e Crystal ball, ref. (93).

^f Ref. (76).

Table 2: $b\bar{b}$ Bound States.

$^3S_1(1^{--})$	Name	Mass (MeV/ c^2)	Γ (MeV) ^a	Γ_{ee} (keV) ^a
1^3S_1	Υ	9460.0 ± 0.2	0.043 ± 0.003	1.22 ± 0.05
2^3S_1	Υ'	10023.4 ± 0.3	0.030 ± 0.007	0.54 ± 0.03
3^3S_1	Υ''	10355.5 ± 0.5	0.0255 ± 0.005^b	0.40 ± 0.03
4^3S_1	Υ'''	10577.5 ± 4.1	$24. \pm 2$	0.24 ± 0.05
5^3S_1	Υ	10864.8 ± 7.9	$110. \pm 13$	0.31 ± 0.07
6^3S_1	Υ	11019.1 ± 8.6	$79. \pm 16$	0.13 ± 0.03

$^3P_J(J^{++})$	Name	Mass (MeV/ c^2)
1^3P_0	χ_{b0}	9859.8 ± 1.3
1^3P_1	χ_{b1}	9891.9 ± 0.7
1^3P_2	χ_{b2}	9913.3 ± 0.6
2^3P_0	χ_{b0}'	10230.5 ± 2.3^c
2^3P_1	χ_{b1}'	10255.7 ± 0.8^c
2^3P_2	χ_{b2}'	10268.6 ± 0.7^c

$^1P_1(1^{+-})$	Name	Mass (MeV/ c^2)
1^1P_1	h_b	9894.8 ± 1.5^d

^a All properties are from Ref. (56) unless otherwise noted.

^b Reference (58).

^c Based on inclusive photon spectra quoted in Ref. (58), and $\Upsilon''(3S)$ mass quoted in Ref. (56).

^d Reference (59).

Table 3: Charmed Hadrons.

J^{PC}	Quark Content	Name	Mass ^a (MeV/ c^2)	Lifetime (10^{-13} sec)	Width ^a (MeV)
<u>Mesons</u>					
0^{-+}	$c\bar{u}$	D^0	1864.6 ± 0.6	$4.3^{+0.2}_{-0.2}$ ^b	
	$c\bar{d}$	D^+	1869.3 ± 0.6	$10.31^{+0.52}_{-0.44}$ ^b	
	$c\bar{s}$	$D_s (F)$	1970.5 ± 2.5	$3.5^{+0.6}_{-0.5}$ ^b	
1^{--}	$c\bar{u}$	D^{*0}	2007.2 ± 2.1		<5
	$c\bar{d}$	D^{*+}	2010.1 ± 0.7		<2
	$c\bar{s}$	$D_s^* (F^*)$	$2113. \pm 8$		
$1^{+2+?}$	$c\bar{d}$	$D (2420)$	$2426. \pm 6$		$75. \pm 20$ ^c
<u>Baryons</u>					
$1/2^+$	cud	Λ_c^+	2281.2 ± 3.0	$1.9^{+0.5}_{-0.3}$ ^b	
	cuu	Σ_c^{++}	$M(\Lambda_c^+) + 168.4 \pm 0.5$ ^d		
	cdd	Σ_c^0	$M(\Lambda_c^+) + 165.8 \pm 0.7$ ^d		
	cus	$\Xi_c^+ (A^+)$	$2460. \pm 25$	$4.8^{+2.9}_{-1.8}$ ^e	
	css	$\Omega_c^0 (T^0)$	$2740. \pm 20$		

^a Properties are from Ref. (56) unless otherwise indicated.

^b Average values from Fig. 8. The precision of these measurements is improving rapidly.

^c Reference (60).

^d Reference (61).

^e Reference (62).

Table 4: *b*-flavored Hadrons.

J^{PC}	Quark Content	Name	Mass (MeV/ c^2)	Lifetime ^a (10^{-13} sec)
<u>Mesons</u>				
0^{-+}	$b\bar{u}$	B^-	$5277.9 \pm 1.1 \pm 3^b$) 14.2 ± 2.7
	$b\bar{d}$	B^0	$5281.0 \pm 0.9 \pm 3^b$	
1^{--}	$b\bar{u}$	B^{*-}) $M(B) + 52.0 \pm 4.5^c$	
	$b\bar{d}$	B^{*0}		

^a Reference (56). The precision of these measurements is improving rapidly.

^b Reference (63).

^c Reference (64).

Table 5. Naive model of light-quark meson and baryon masses described in text.

J^P	Meson	Mass (MeV/c ²)		J^P	Baryon	Mass (MeV/c ²)	
		Calculated ^a	Measured			Calculated ^b	Measured
0 ⁻	π	140	138		N	939	938
	K	485	496	1/2 ⁺	Λ	1114	1116
	η	559	549		Σ	1179	1195
	ρ	780	776		Ξ	1327	1318
1 ⁻	ω	780	783		Δ	1239	1232
	K^*	896	892	3/2 ⁺	Σ^*	1381	1385
	ϕ	1032	1020		Ξ^*	1529	1533
					Ω	1682	1672

$$^a m_U = m_D = 310 \text{ MeV}/c^2; m_S = 483 \text{ MeV}/c^2; \Delta E_{SS} = (160 \text{ MeV}/c^2) \times \sigma_i \sigma_j (m_U^2/m_i m_j)$$

$$^b m_U = m_D = 363 \text{ MeV}/c^2; m_S = 538 \text{ MeV}/c^2; \Delta E_{SS} = (100 \text{ MeV}/c^2) \times \sigma_i \sigma_j (m_U^2/m_i m_j)$$

Table 6. Lowest order expressions and first order QCD corrections for decay processes of $c\bar{c}$ and $b\bar{b}$.

Process	Rate ^a	Correction factor	
$n^3S_1 \rightarrow e^+e^-$	$\frac{16\pi}{3} N_c \alpha^2 e_Q^2 \Psi(0) ^2 / M_n^2$	$1 - 16 \alpha_s / 3\pi$	(3.17)
$\rightarrow \gamma\gamma\gamma$	$\frac{16(\pi^2 - 9)}{9} N_c \alpha^3 e_Q^6 \Psi(0) ^2 / m_Q^2$	$1 - 12.6 \alpha_s / \pi$	(3.18)
$\rightarrow ggg$	$\frac{40(\pi^2 - 9)}{81} \alpha_s^3 \Psi(0) ^2 / m_Q^2$	$1 + 4.9 \alpha_s / \pi$ for J/ψ $1 + 3.8 \alpha_s / \pi$ for Υ	(3.19) ^a
$\rightarrow gg\gamma$	$\frac{32(\pi^2 - 9)}{9} e_Q^2 \alpha \alpha_s^2 \Psi(0) ^2 / m_Q^2$	$1 - 0.9 \alpha_s / \pi$ for J/ψ $1 - 1.7 \alpha_s / \pi$ for Υ	
$n^1S_0 \rightarrow \gamma\gamma$	$4\pi N_c e_Q^4 \alpha^2 \Psi(0) ^2 / m_Q^2$	$1 - 3.4 \alpha_s / \pi$	(3.21)
$\rightarrow gg$	$\frac{8\pi}{3} \alpha_s^2 \Psi(0) ^2 / m_Q^2$	$1 + 10.6 \alpha_s / \pi$ for η_c $1 + 10.2 \alpha_s / \pi$ for η_b	(3.22) ^a
$n^3P_2 \rightarrow \gamma\gamma$	$\frac{12}{5} N_c e_Q^4 \alpha^2 R'_{nP}(0) ^2 / m_Q^4$	a	
$\rightarrow gg$	$\frac{8}{5} \alpha_s^2 R'_{nP}(0) ^2 / m_Q^4$	$(1 + 8.4 \alpha_s / \pi) a$ for χ $(1 + 11.7 \alpha_s / \pi) a$ for χ_b	(3.24) ^a
$n^3P_1 \rightarrow q\bar{q}g$	$\frac{8}{9\pi} n_f \alpha_s^3 \ln(2m_Q \langle r \rangle) R'_{nP}(0) ^2 / m_Q^4$	not known	
$n^3P_0 \rightarrow \gamma\gamma$	$9N_c e_Q^4 \alpha^2 R'_{nP}(0) ^2 / m_Q^4$	$(1 + 5.5 \alpha_s / \pi) a$	(3.26)
$\rightarrow gg$	$6 \alpha_s^2 R'_{nP}(0) ^2 / m_Q^4$	$(1 + 20.4 \alpha_s / \pi) a$ for χ $(1 + 21.2 \alpha_s / \pi) a$ for χ_b	(3.27) ^a

^a N_c is the number of quark colors. Rate expressions that do not contain a factor of N_c are for $N_c = 3$. For $N_c = (6, 8)$, the rate expressions in 3.20, 3.22, 3.24, 3.27 should be multiplied by a factor of $(25/2, 27/2)$, and 3.19 by $(49/2, 0)$.

^b The absolute magnitude of the P-states corrections are not yet known; only ratios have been calculated.

^c n_f is the number of light quark flavors.

HEAVY QUARK SYSTEMS

Table 7. Discrete states reached in radiative decays of J/ψ

State ^a	Mass (MeV/c ²)	J^P	Final state(s)	J/ψ branching ratio (%)	Remarks
π^0	135	0^-	All	0.004 ± 0.001	1S_0 $q \bar{q}$ state
η	549	0^-	All	0.086 ± 0.008	"
η'	958	0^-	All	0.42 ± 0.05	"
$f_2(f)$	1274	2^+	All	0.16 ± 0.02	3P_2 $q \bar{q}$ state
$\eta(1)$	1440	0^-	$K \bar{K} \pi$ All	0.46 ± 0.07 $> 0.69 \pm 0.11$	Glueball candidate
$f_2'(f')$	1525	2^+	All	0.016 ± 0.005	3P_2 $q \bar{q}$ state
$f_2(\theta)$	1716	2^+	$\eta \eta$ $K \bar{K}$ $\pi \pi$	0.026 ± 0.011^b 0.096 ± 0.014^b 0.020 ± 0.004^b	Glueball candidate
$X(\xi)$	2232	$2^{+?}$	$K^+ K^-$ $K_s K_s$	0.0084 ± 0.0032 0.013 ± 0.007	Interpretation unknown
η_c	2981	0^-	All	1.27 ± 0.36	1S_0 $c \bar{c}$ state

^a Where different from the Particle Data Group nomenclature, the common name of the state is shown in parentheses. Branching ratios are from (56) unless otherwise noted.

^b Averages quoted in (42).

Table 8. E1 transitions in $c\bar{c}$ systems

Transition	Photon energy (MeV)	Experimental branching ratio (%) ^a	Expt ^b	Partial decay rate (keV)		
				MR(87)	MB(88)	GRR(89) ^d
$2S \rightarrow 1^3P_2$	128	7.8 ± 0.8	17 ± 4	41 (39)	27 (27)	24 (33)
	1^3P_1	8.7 ± 0.8	19 ± 4	48 (51)	31 (40)	35 (49)
	1^3P_0	9.4 ± 0.8	20 ± 4	37 (54)	19 (45)	44 (64)
$1^3P_2 \rightarrow J/\psi$	429	14.8 ± 1.7	385^{+212}_{-155}	609 (495)	347 (362)	502 (753)
$1^3P_1 \rightarrow J/\psi$	389	25.8 ± 2.5	< 355	460 (368)	270 (250)	369 (562)
$1^3P_0 \rightarrow J/\psi$	303	0.7 ± 0.2	147 ± 38	226 (174)	128 (121)	171 (253)

^aFrom compilation of (56)

^bBased on total widths (76,93) of $2.6^{+1.4}_{-1.0}$, <1.3 , and 13-21 MeV for $^3P_{2,1,0}$ states, respectively

^cNonrelativistic predictions are shown in parentheses below the relativistically corrected values

^d1985 values. Substantial changes occur in 1986 work.

HEAVY QUARK SYSTEMS

Table 9. M1 transitions in charmonium

Decay	Partial width (keV)	Photon energy (MeV)	Overlap $\langle f j_0(E_\gamma r/2) i \rangle$	
			Experiment ^a	Theory
$J/\psi \rightarrow \eta_c \gamma$	0.80 ± 0.25	114	0.64 ± 0.10	0.9975
$\psi' \rightarrow \eta_c' \gamma$	0.4 - 2.8	91 ± 5	0.64 - 1.67	0.9925
$\psi' \rightarrow \eta_c \gamma$	0.60 ± 0.17	638	0.042 ± 0.006	0.066
$\eta_c' \rightarrow J/\psi \gamma$	—	463	—	0.037

^aExtracted from (3.14) with $m_c = 1.8 \text{ GeV}/c^2$

HEAVY QUARK SYSTEMS

Table 10. Charmed hadron masses in a model with additive and hyperfine contributions.

J^P	Meson	Mass (MeV/c ²)	
		Predicted ^a	Observed ^b
0 ⁻	$D = c\bar{u}, c\bar{d}$	1882	1867
	$D_s = c\bar{s}$	2088	1971
1 ⁻	$D^* = c\bar{u}, c\bar{d}$	2002	2009
	$D_s^* = c\bar{s}$	2164	2113
J^P	Baryon	Mass (MeV/c ²)	
		Predicted ^c	Observed ^b
1/2 ⁺	$\Lambda_c^+ = udc$	2281 (input)	2281 ± 3
	$\Sigma_c = uuc, udc, ddc$	2438	2448 ± 4 ^d
	$\Xi_c = usc, dsc$	2505 ^e	2460 ± 25
		2604 ^f	
	$\Omega_c = ssc$	2775	2740 ± 20
3/2 ⁺	$\Sigma_c^* = uuc, udc, ddc$	2502	
	$\Xi_c^* = usc, dsc$	2658	
	$\Omega_c^* = ssc$	2818	

^a $m_c = 1662 \text{ MeV}/c^2$; other parameters as in Table 5

^b Masses are from (56) unless noted otherwise

^c $m_c = 1705 \text{ MeV}/c^2$; other parameters as in Table 5

^d Ref. (60)

^e State antisymmetric under exchange of s and u

^f State symmetric under exchange of s and u

Table 11. Partial decay modes of the Υ

Decay mode	Branching ratio (%)	Partial width (keV)
$e^+ e^-$	2.82 ± 0.31	1.22 ± 0.05
$\mu^+ \mu^-$	2.78 ± 0.22	1.20 ± 0.05
$\tau^+ \tau^-$	2.76 ± 0.2^a	1.19 ± 0.05^a
$\gamma^* \rightarrow q \bar{q}$	10.3 ± 1.0^a	4.42 ± 0.55^a
$\gamma g g$	1.62 ± 0.43^b	0.70 ± 0.19
$g g g$	79.8 ± 1.4	34.4 ± 2.5
	100	43.1 ± 3.1

^aCalculated value

^bFrom ratio $\Gamma(\gamma g g)/\Gamma(g g g) = 2.03 \pm 0.53 \% (109)$.

HEAVY QUARK SYSTEMS

Table 12. Partial decay modes of the $\Upsilon(2S)$ level

Decay mode	Branching ratio (%)	Partial width (keV)
$e^+ e^-$	1.52 ± 0.13	0.537 ± 0.033^a
$\mu^+ \mu^-$	1.52 ± 0.13	0.537 ± 0.033
$\tau^+ \tau^-$	1.51 ± 0.13	0.534 ± 0.033
$\gamma^* \rightarrow q \bar{q}$	5.6 ± 0.5	1.97 ± 0.12
$\Upsilon \chi_{b0}$	4.31 ± 0.96^a	1.52 ± 0.38
$\Upsilon \chi_{b1}$	6.73 ± 0.86^a	2.38 ± 0.39
$\Upsilon \chi_{b2}$	6.57 ± 0.87^a	2.32 ± 0.39
$\Upsilon \pi^+ \pi^-$	18.75 ± 0.99^a	6.62 ± 0.78
$\Upsilon \pi^0 \pi^0$	9.37 ± 0.50	3.31 ± 0.39
$\gamma g g$	0.88 ± 0.23	0.31 ± 0.09
$g g g$	43.28 ± 1.94	15.28 ± 1.74
	100	35.3 ± 3.7

^aBased on compilation of (56). All other values are calculated on the basis of Eq. (5.4) as explained in the text.

Table 13. Partial decay modes of the $\Upsilon(3S)$ level

Decay mode	Branching ratio (%)	Partial width (keV)
$e^+ e^-$	1.72 ± 0.20	0.402 ± 0.031^a
$\mu^+ \mu^-$	1.72 ± 0.20	0.402 ± 0.031
$\tau^+ \tau^-$	1.71 ± 0.20	0.400 ± 0.031
$\gamma^* \rightarrow q \bar{q}$	6.3 ± 0.5	1.47 ± 0.11
$\Upsilon \chi_{b0}(2P)$	5.3 ± 2.3^b	1.24 ± 0.54
$\Upsilon \chi_{b1}(2P)$	11.7 ± 3.0^b	2.73 ± 0.80
$\Upsilon \chi_{b2}(2P)$	12.8 ± 3.3^b	2.99 ± 0.88
$\Upsilon(1S) \pi^+ \pi^-$	3.47 ± 0.34^c	0.81 ± 0.14
$\Upsilon(1S) \pi^0 \pi^0$	1.74 ± 0.17	0.41 ± 0.07
$\Upsilon(2S) \pi^+ \pi^-$	2.1 ± 0.5^c	0.49 ± 0.14
$\Upsilon(2S) \pi^0 \pi^0$	1.05 ± 0.25	0.25 ± 0.07
$\Upsilon(1^1P_1) \pi^+ \pi^-$	0.37 ± 0.15^c	0.09 ± 0.04
$\Upsilon(1^1P_1) \pi^0 \pi^0$	0.19 ± 0.08	0.04 ± 0.02
$\gamma g g$	0.88 ± 0.23	0.21 ± 0.06
$g g g$	48.86 ± 5.1	11.42 ± 1.99
	100	23.37 ± 3.26

^aBased on compilation of (56).

^bRef. (58)

^cRef. (59)

All other values are calculated on the basis of Eq. (5.4) as explained in the text.

HEAVY QUARK SYSTEMS

Table 14. Predictions for $\Delta M \equiv M(\chi_b^j) - \langle M(\chi_b^j) \rangle$ of a scalar confinement model

State	$\Delta M(\chi_b[1P]), \text{MeV}/c^2$		$\Delta M(\chi_b'[2P]), \text{MeV}/c^2$	
	Predicted ^a	Observed ^b	Predicted ^a	Observed ^c
3P_0	-39.3	-40.4 ± 1.4	-29.4	-29.6 ± 2.4
3P_1	-8.6	-8.3 ± 0.8	-6.5	-4.4 ± 1.0
3P_2	13.0	13.1 ± 0.7	9.8	8.5 ± 0.9
$\frac{M(\chi_2) - M(\chi_1)}{M(\chi_1) - M(\chi_0)}$	0.71	0.67 ± 0.06	0.71	0.57 ± 0.06^d

^a Ref. (127)^b Ref. (56)^c Ref. (58)^dBased on combination of inclusive and exclusive photon spectra in (58)

HEAVY QUARK SYSTEMS

Table 15. E1 transitions in $b\bar{b}$ systems.

Transition	Photon energy (MeV)	Experimental branching ratio (%)	Partial decay width (keV)	
			Experiment	Theory ^a
2S → 1 ³ P ₂	109.5±0.6	6.57 ± 0.87	1.97 ± 0.55 ^b	2.1
	130.7±0.7	6.73 ± 0.86	2.02 ± 0.55 ^b	2.2
	162.3±1.3	4.31 ± 0.96	1.29 ± 0.43 ^b	1.4
1 ³ P ₂ → γ	444.2±2.4	22.0 ± 4.2	29.2 ± 5.6 ^c	38
1 ³ P ₁ → γ	425.0 ± 3.5	35.0 ± 8.0	22.4 ± 5.1 ^c	33
1 ³ P ₀ → γ	404.3±5.8	< 6	< 22.9 ^c	29
3S → 2 ³ P ₂	86.5±0.7	12.8 ± 3.3	3.3 ± 1.1 ^d	2.8
	99.3±0.8	11.7 ± 3.0	3.0 ± 1.0 ^d	2.5
	124.2±2.3	5.3 ± 2.3	1.4 ± 0.7 ^d	1.6
1 ³ P ₂	431.5±2.4	-	-	0.025
1 ³ P ₁	450.7±3.5	-	-	0.017
1 ³ P ₀	471.4±5.8	-	-	0.006
2 ³ P ₂ → γ'	244.6±2.4	15 ± 8	17 ± 9 ^e	19.2
	γ	778.9±2.4	16 ± 6	19 ± 7 ^e
2 ³ P ₁ → γ'	227.7±3.4	24 ± 10	14 ± 6 ^e	15.5
	γ	763.1±3.4	7 ± 3	4.2 ± 1.8 ^e
2 ³ P ₀ → γ'	207.3±5.8	4 ± 3	13 ± 10 ^e	11.7
	γ	743.7±5.8	<3 (90% c.l.)	<10 ^e

^aSee (127)^bBased on total width of 2S level quoted in (56)^cBased on calculated total widths of (132, 64, 382) keV for $J = 2, 1, 0$ ^dBased on total width of 3S level quoted in (58)^eBased on calculated total widths of (116, 60, 336) keV for $J = 2, 1, 0$

FIGURE CAPTIONS

Fig. 1. Initial evidence for the J/ψ . a) Hadronic production in the reaction $p + Be \rightarrow e^+e^- + \text{anything}$ (11). b) Formation in electron-positron annihilations (12).

Fig. 2. Evidence for the Υ . a) Initial mass spectrum (23); b) A recent spectrum in hadronic production (24).

Fig. 3. Charmonium ($c\bar{c}$) spectrum. Arrows denote decays and are labeled by branching ratios, in percent. The band at mass = $2M(D)$ denotes the flavor threshold, above which levels are broader than those below it.

Fig. 4. Spectrum of the upsilon ($b\bar{b}$) family. Arrows are labeled by branching ratios to specific channels, in percent. Levels above flavor threshold (band at mass = $2M(B)$) are broader than levels below it.

Fig. 5. Chromoelectric lines of force for the Interquark interaction at a) short, and b) long distances.

Fig. 6. Possible mechanisms for hadronic production of quarkonium states. a) Two-gluon fusion and subsequent electromagnetic decay; b) Quark-antiquark annihilation; c) Direct-channel production of a quarkonium state in proton-antiproton annihilations.

Fig. 7. Graphs describing production of 0^-1^- pairs in J/ψ decays. a) Three-gluon intermediate state; b) One-photon intermediate state.

HEAVY QUARK SYSTEMS

Fig. 8. Compilation of charmed particle lifetime measurements. a) D^0 ; b) D^+ ; c) D_S ; d) Λ_c .

Fig. 9. Electromagnetic transitions giving rise to $1^3D_{1,2,3}$ states. a) from the 3^3S_1 , b \bar{b} level; b) from the 3^3P levels, capable of giving rise both to the 3^3S_1 state [the $\Upsilon(3S)$] and to 2^3D levels.

Fig. 10. $L = 0$ mesons and baryons containing a single b -flavored quark. Adapted from Ref. 3.

Fig. 11. Comparison of potentials constructed via the inverse-scattering method from Υ levels (heavy curve, levels on left) and charmonium levels (light curve, levels on right).

Fig. 12. Ratios of level spacings implied by power-law potentials behaving as r^V . a) $(E_{3S} - E_{2S})/(E_{2S} - E_{1S})$; b) $(E_{4S} - E_{3S})/(E_{3S} - E_{2S})$; c) $(E_{2S} - E_{1P})/(E_{2S} - E_{1S})$; d) $(E_{3S} - E_{2P})/(E_{3S} - E_{2S})$. [ψ : + ; Υ : o.]

Fig. 13. Comparison of predicted $c \bar{c}$, $b \bar{b}$, and $Q \bar{Q}$ levels (for $m_Q = 40 \text{ GeV}/c^2$) in the potential (solid curve) of Ref. (87). For $Q \bar{Q}$ levels, both the energy and average radius are shown. The dashed curve describes $V(r) = (8\pi/27)(\lambda r - 1)^2/r \ln \lambda r$, $\lambda = 0.7325 \text{ GeV}$ (134).

Fig. 14. Expected decay rates and branching ratios of 1S–3S levels of toponium. [From Kühn and Ono (138) potential "T."] $F \bar{F}$: fermion pairs via virtual γ and Z ; SQD: charged current decay of a single t -quark. The results for the Richardson potential(67) are very similar (see the erratum in (138).)

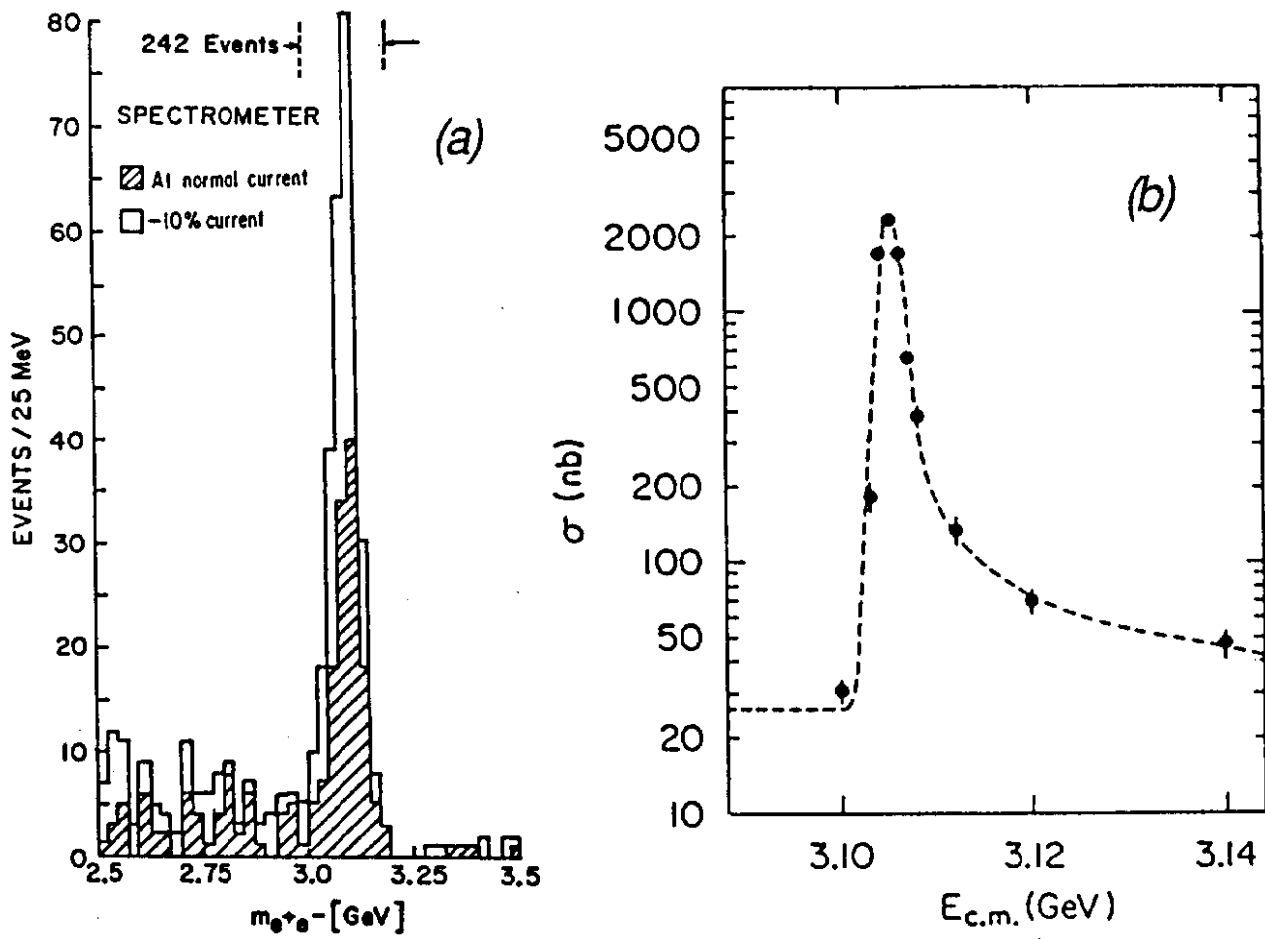


Figure 1

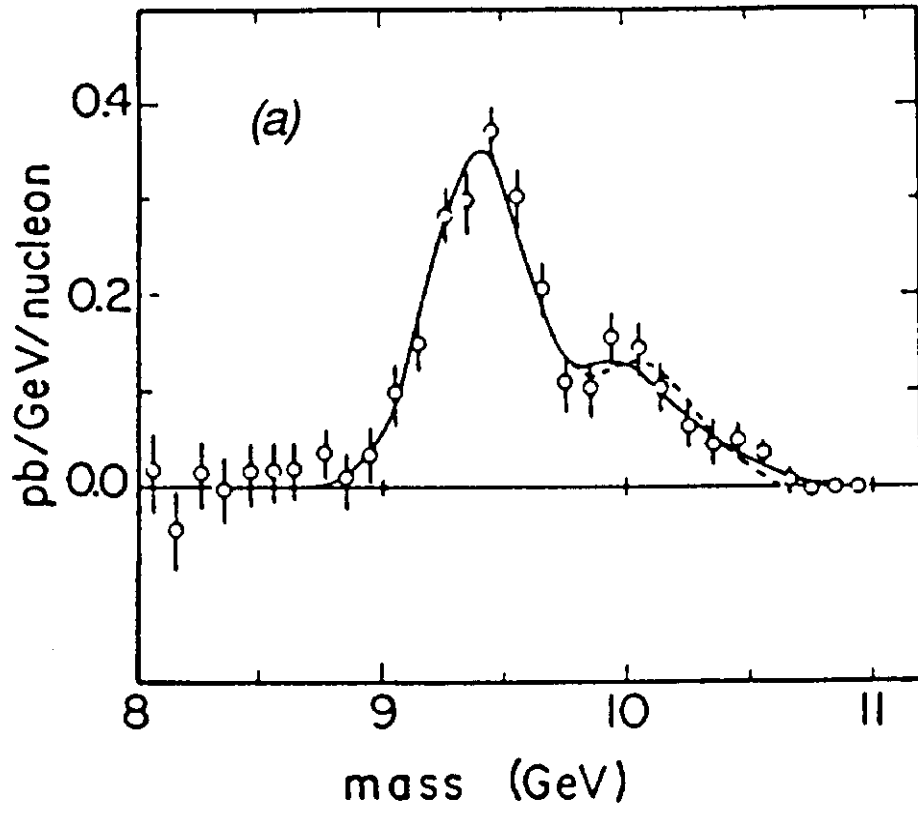


Figure 2a

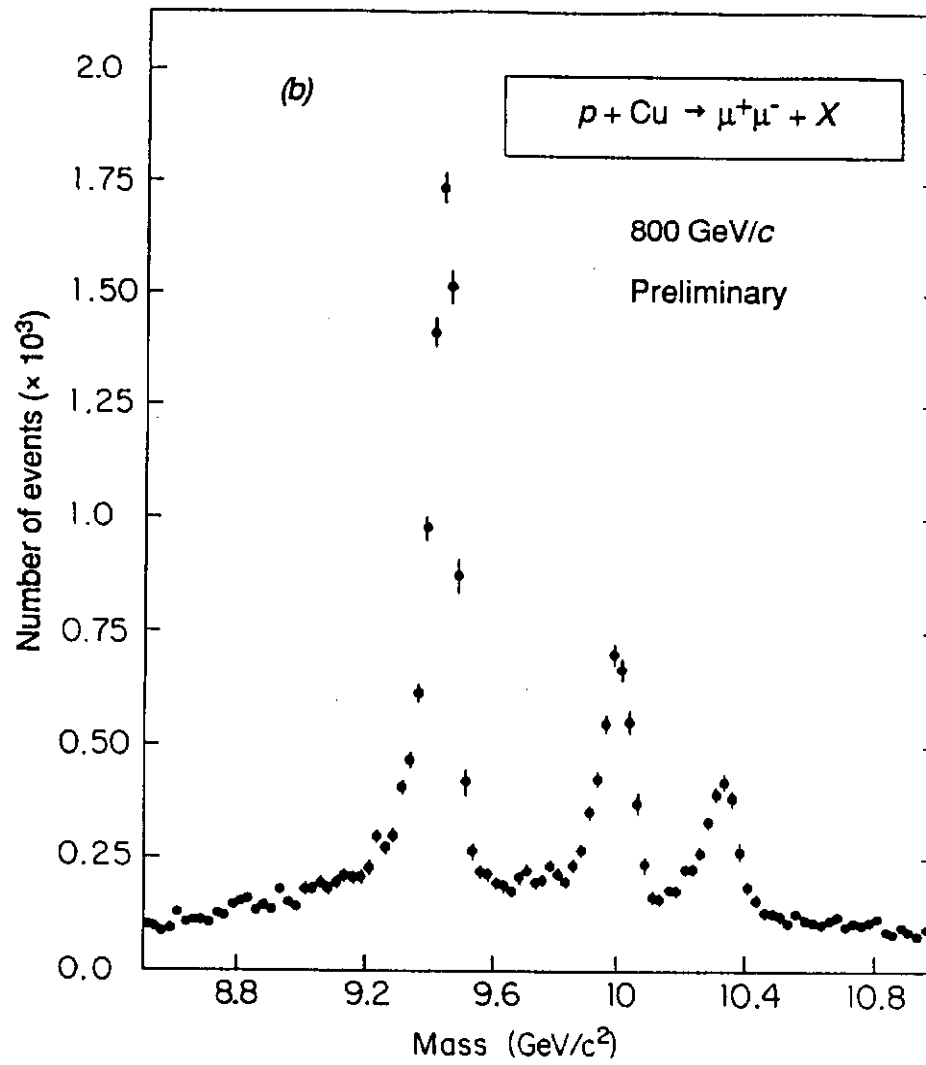


Figure 2b

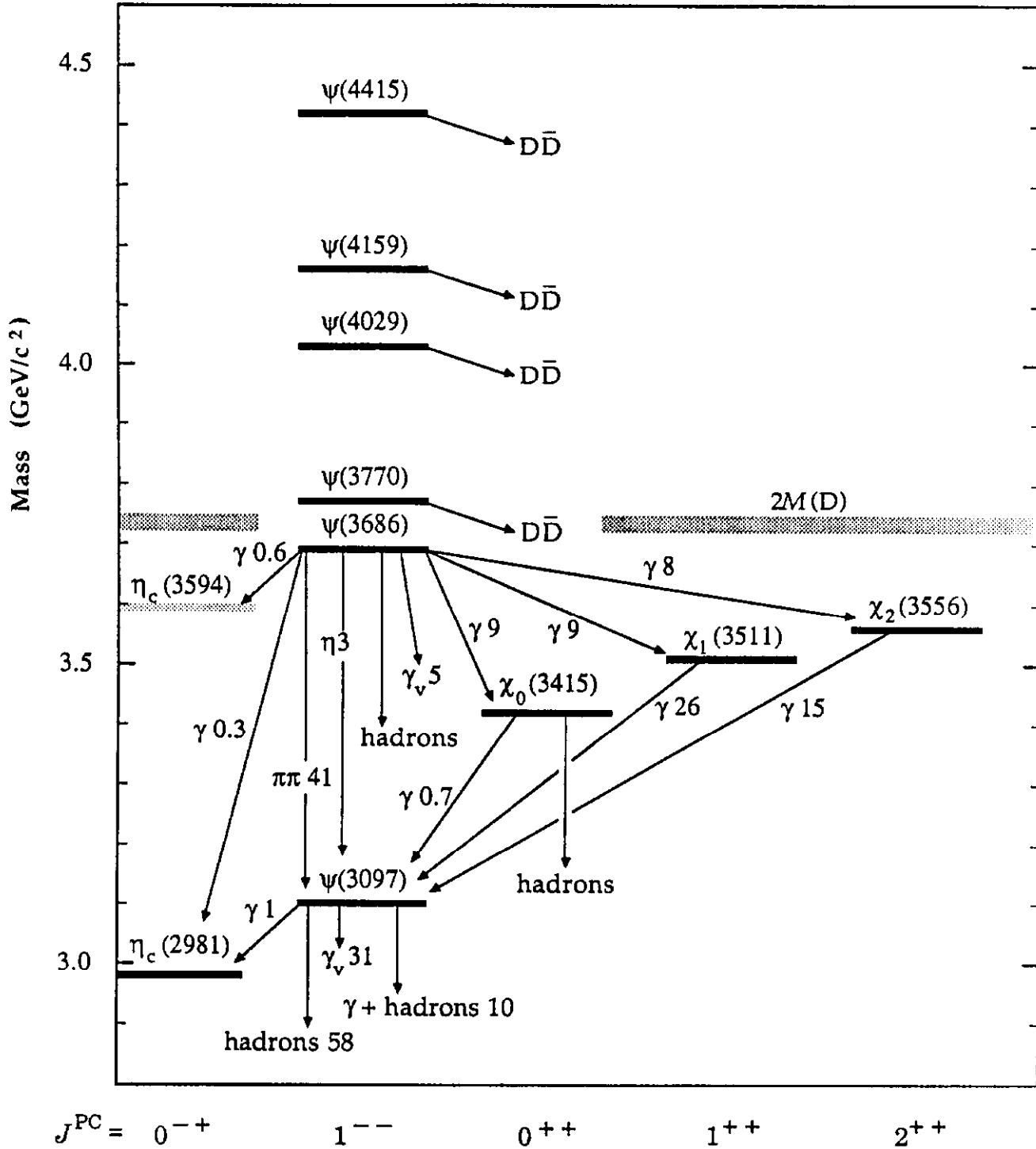


Figure 3

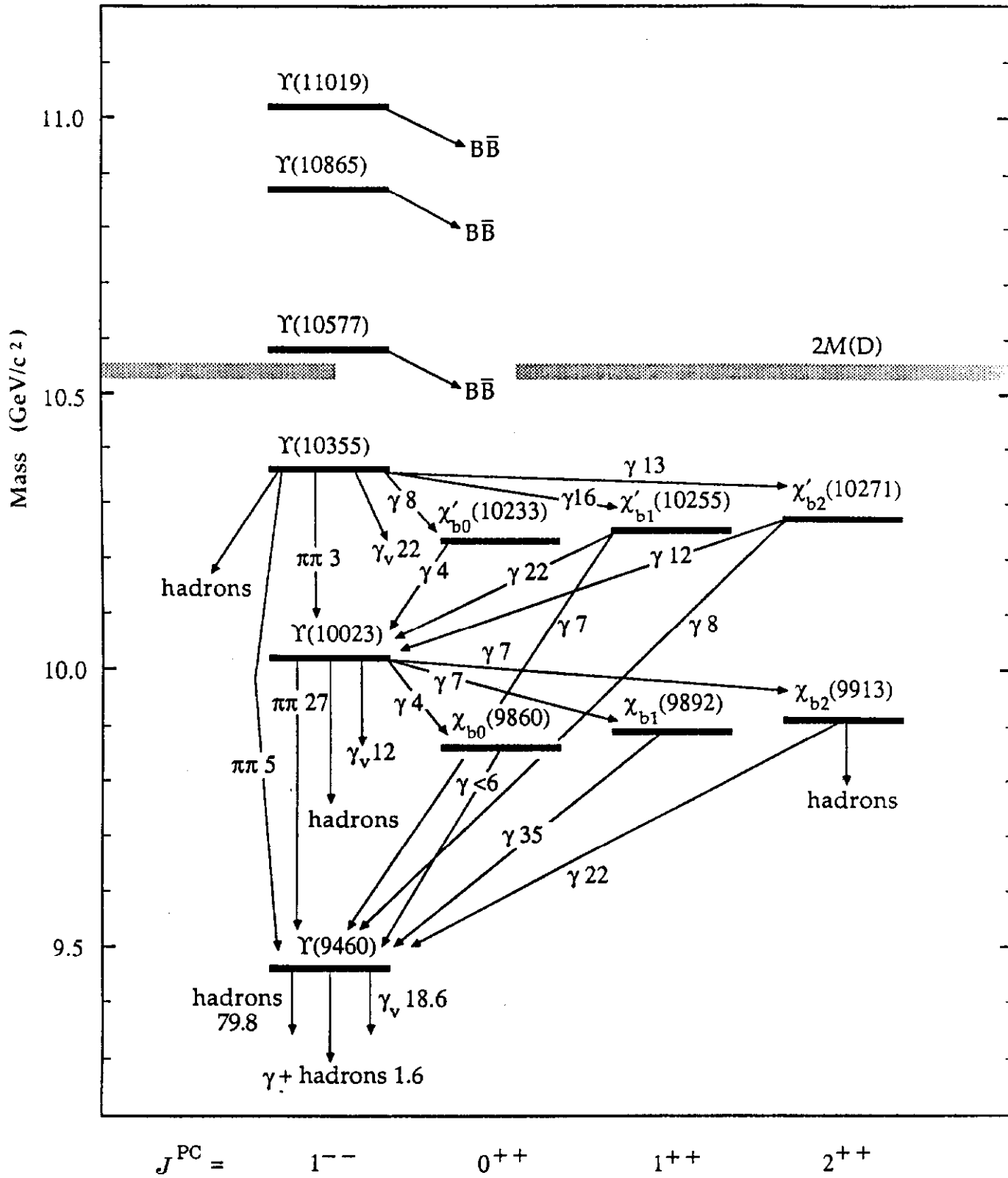


Figure 4

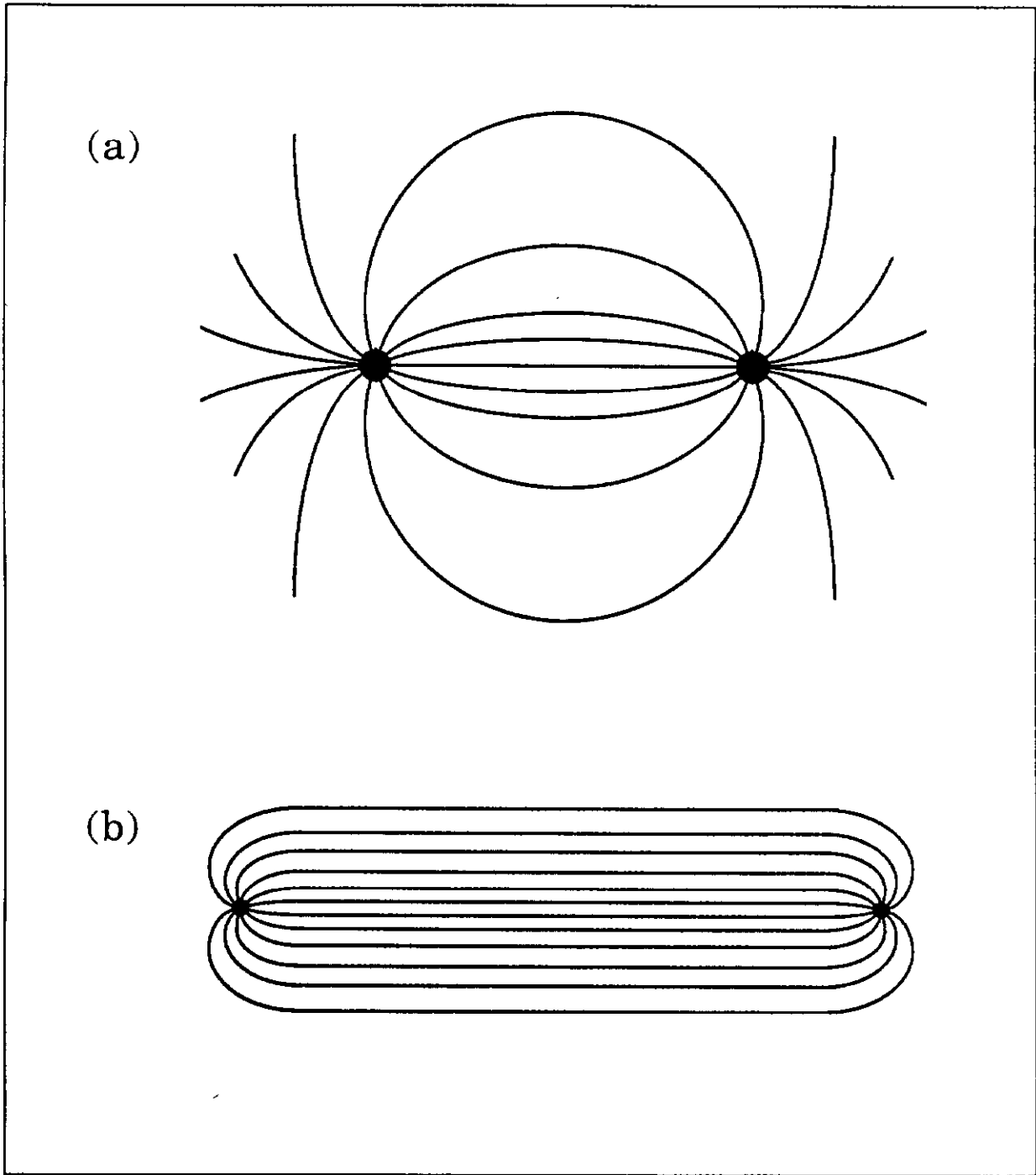


Figure 5

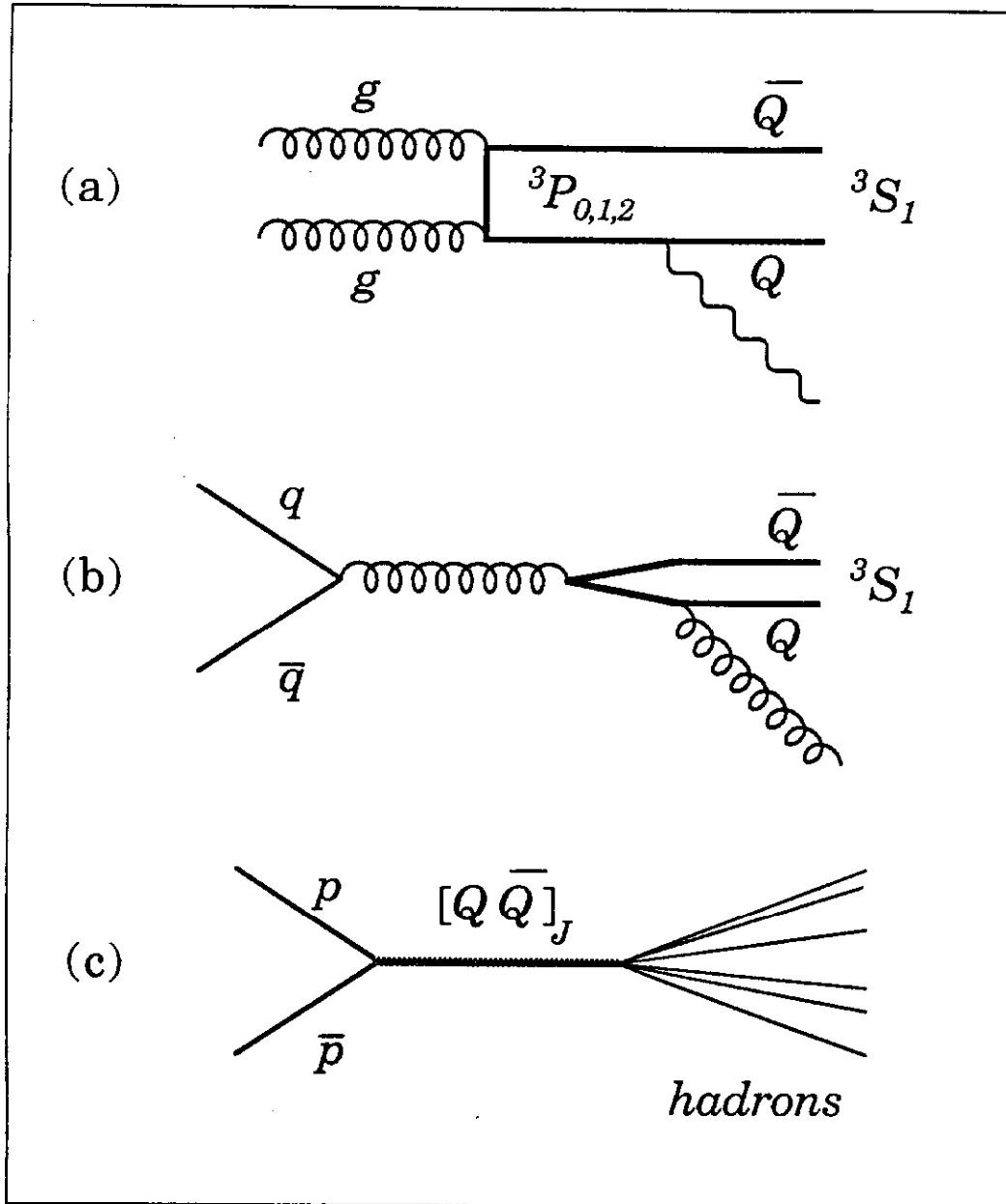


Figure 6

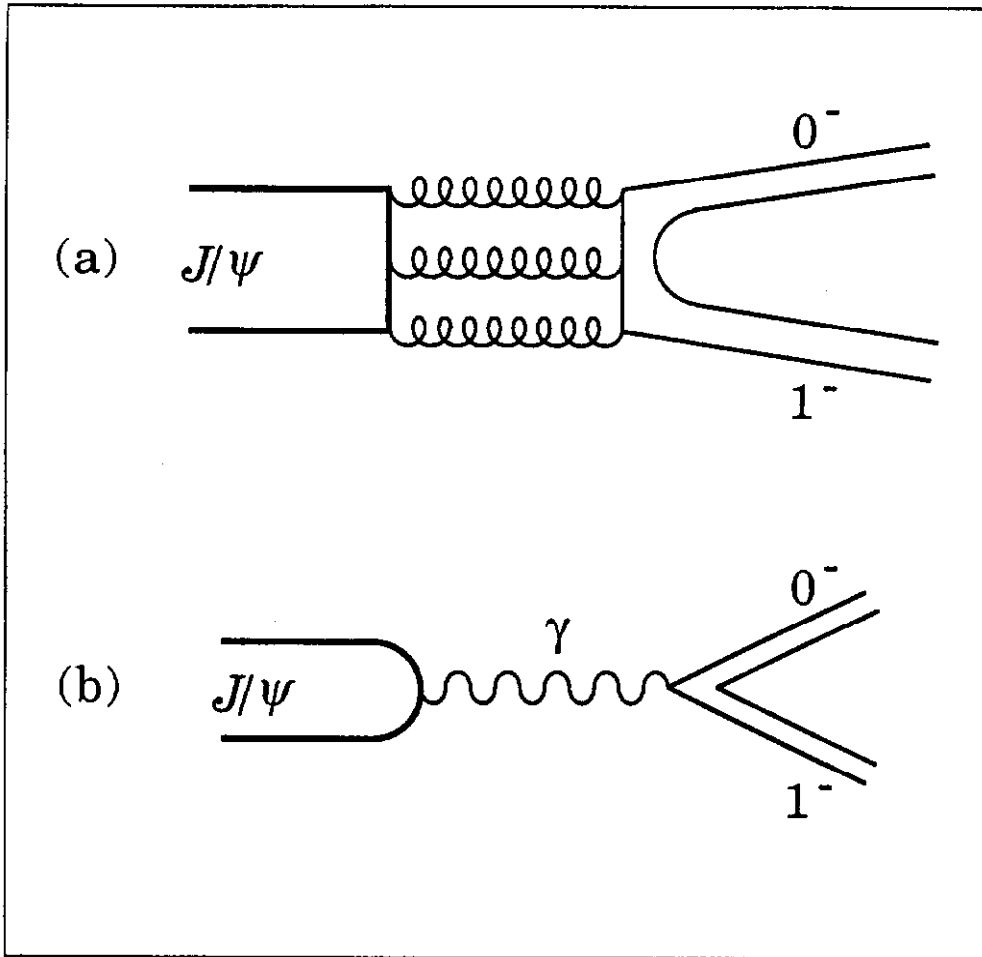


Figure 7

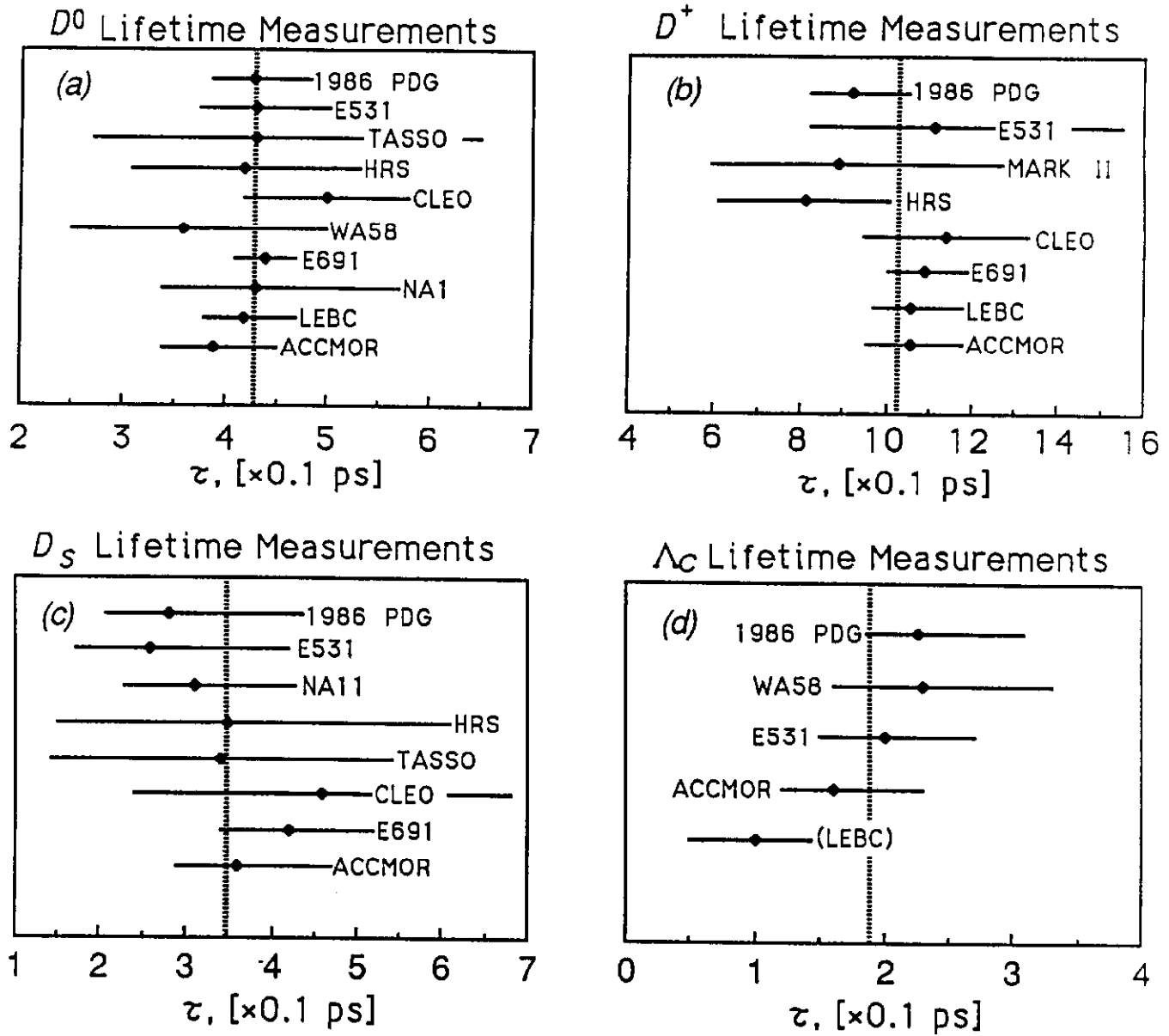


Figure 8

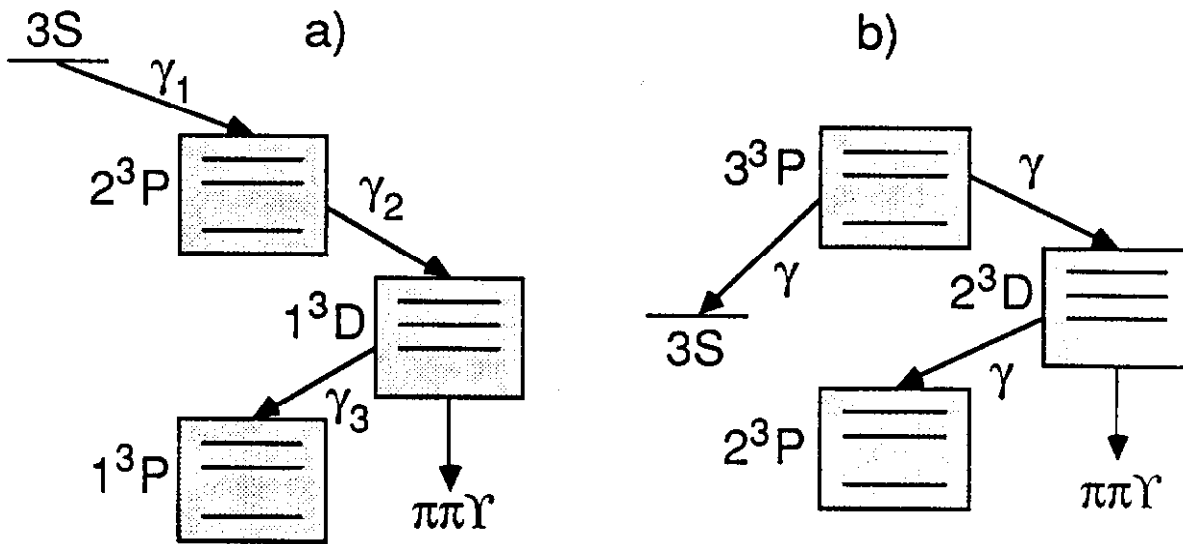


Figure 9

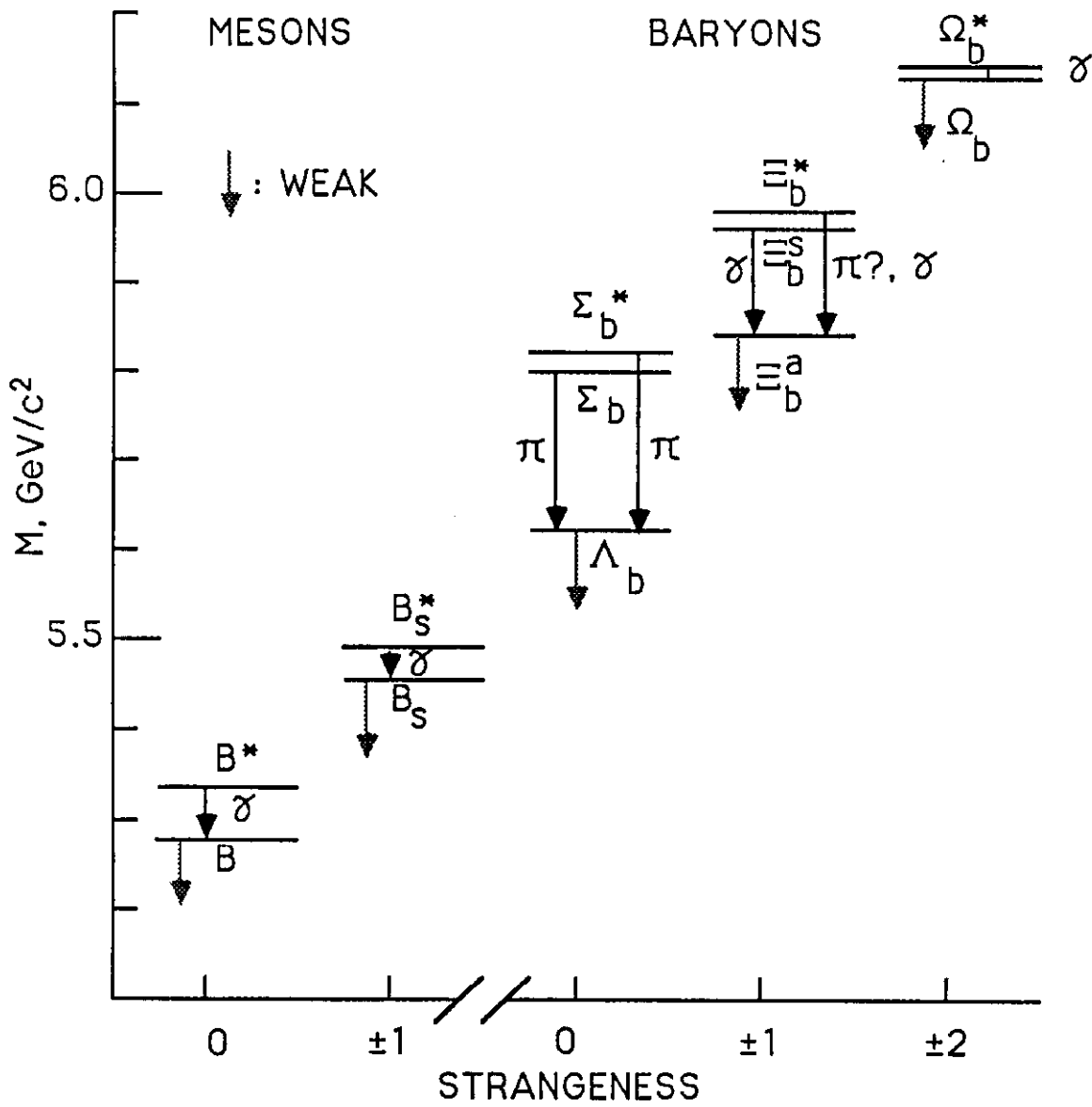


Figure 10

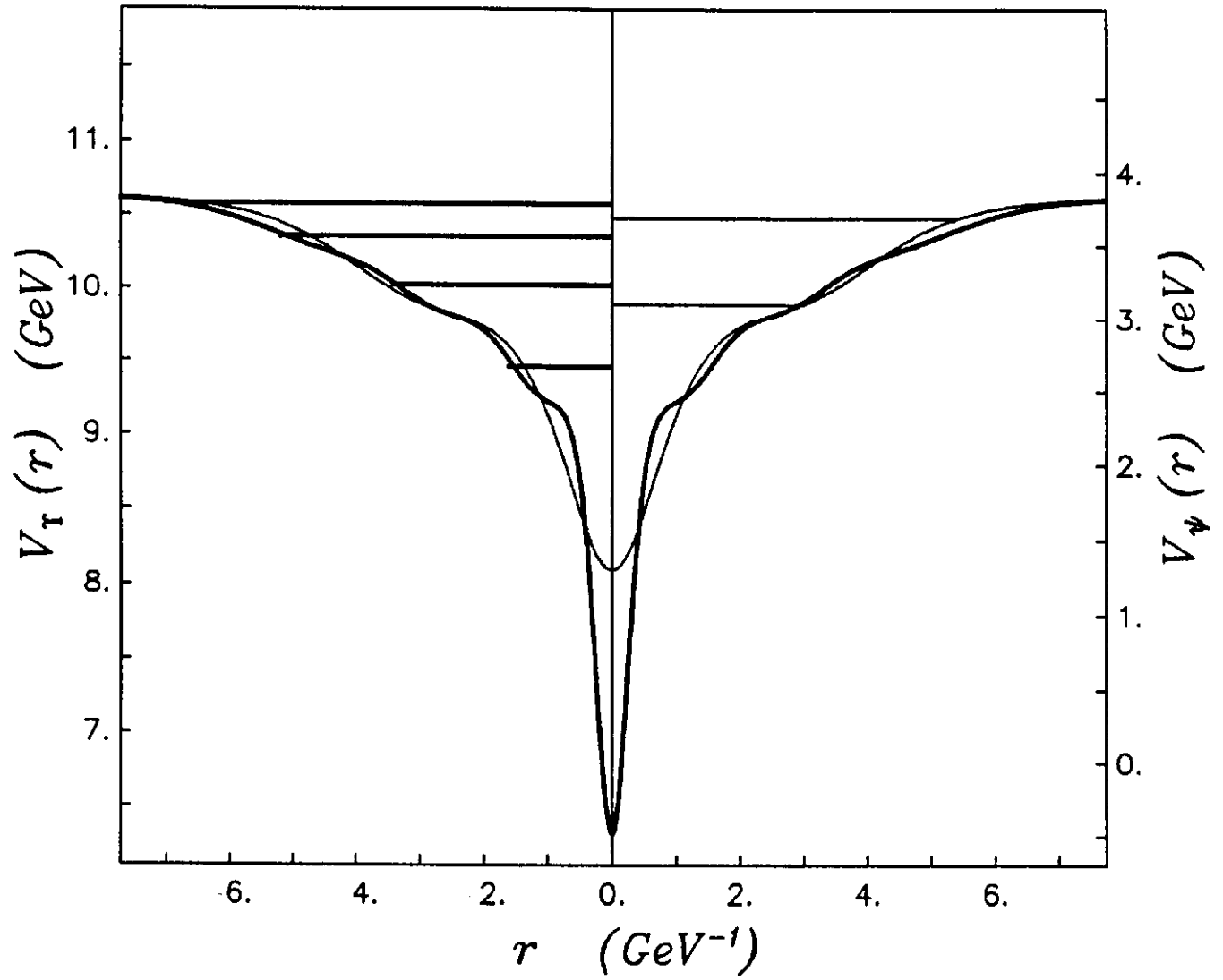


Figure 11

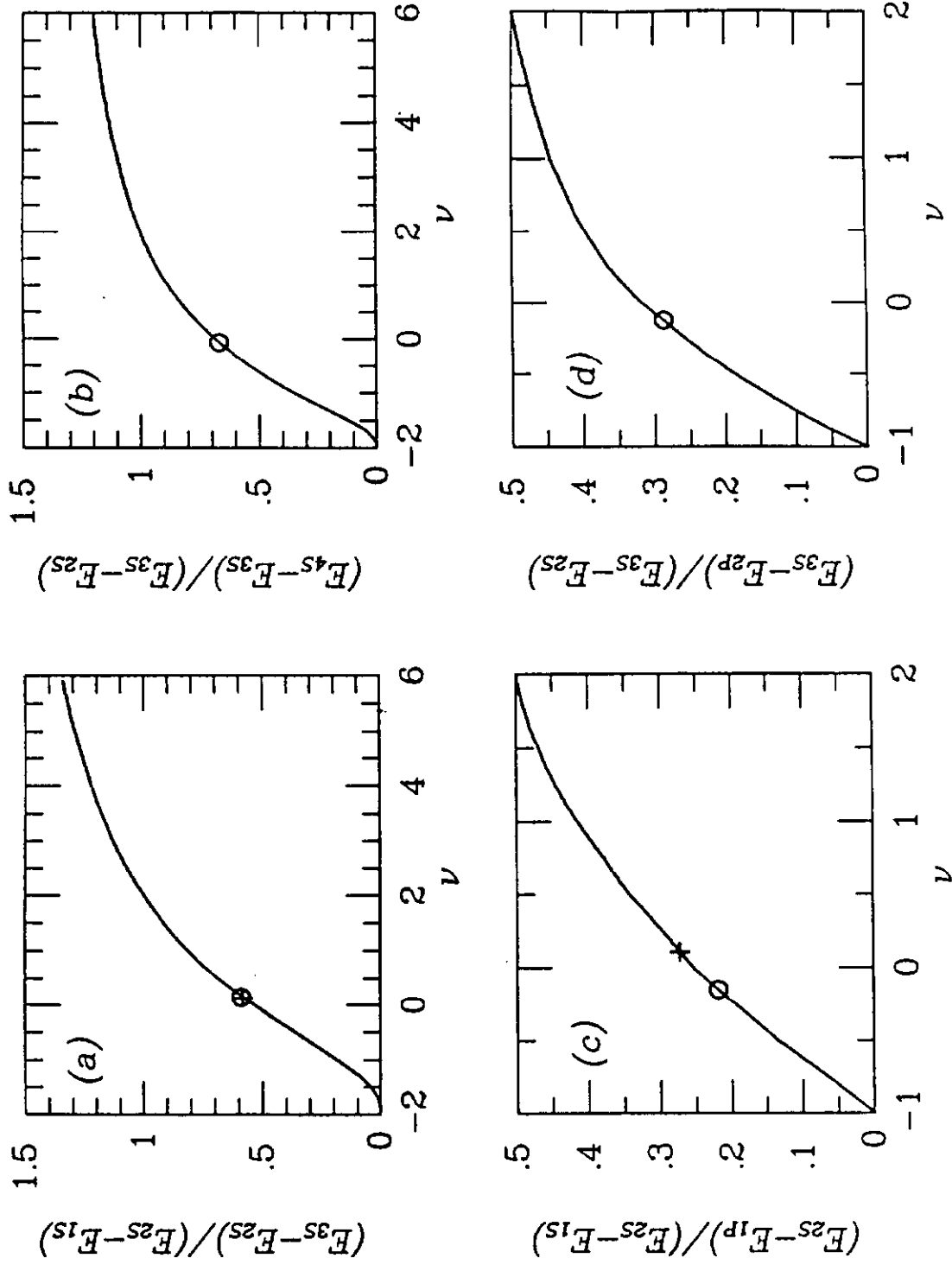


Figure 12

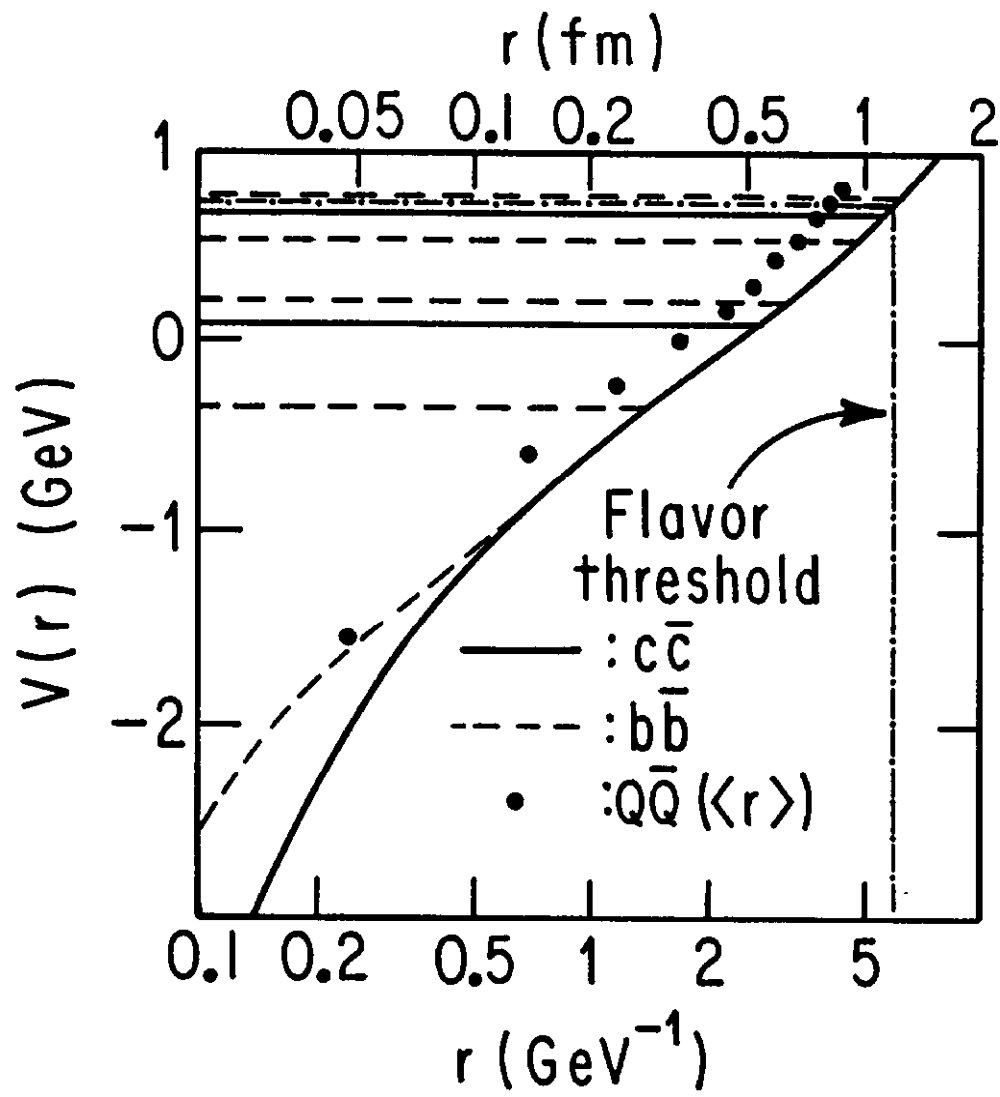


Figure 13

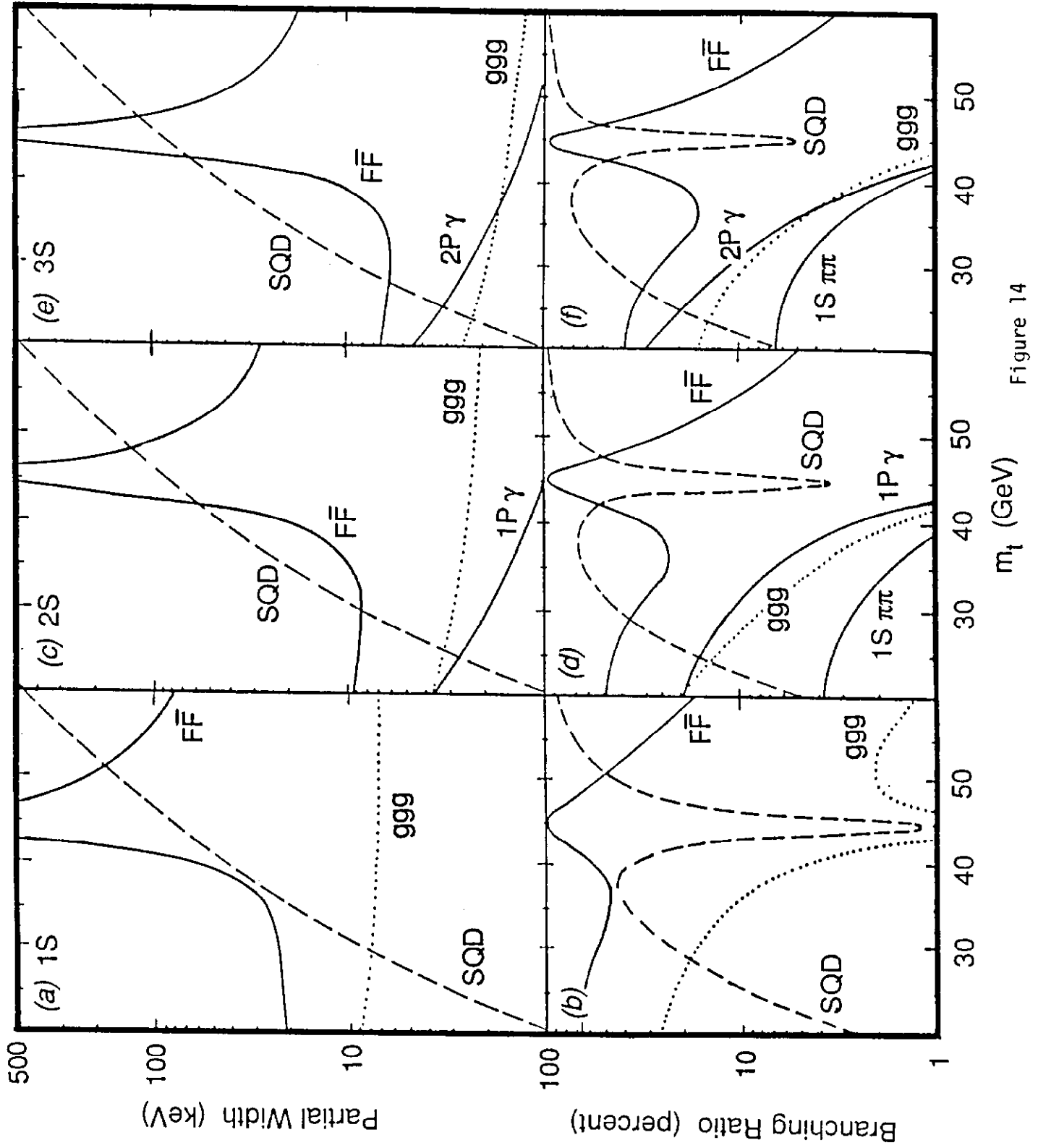


Figure 14